PULL OUT BEHAVIOUR OF STRIP PLATE ANCHORS IN CLAY BY NUMERICAL MODELLING

BY

PRASUN CHANDRA PRAMANICK

REGISTRATION NO. – 128863 of 2014 -15

EXAMINATION ROLL NO. – M4CIV1604

Under the Guidance of

PROF. SIBAPRIYA MUKHERJEE

Department of Civil Engineering

A thesis to be

Submitted in Partial Fulfilment of the Requirements

For the degree of

Master of Civil Engineering in Soil Mechanics and Foundation Engineering

Department of Civil Engineering

Faculty of Engineering & Technology

Jadavpur University

Kolkata – 700 032

May, 2016

Declaration of Originality and Compliance of Academic Ethics

I hereby declare that this thesis contains literature survey and original research work by the undersigned candidate, as part of his **Master of Civil Engineering in Soil Mechanics & Foundation engineering studies.**

All information in this document have been obtained and presented in accordance with academic rules and ethical conduct.

I also declare that, as required by these rules and conduct, I have fully cited and referenced all material and results that are not original to this work.

Name : Prasun Chandra Pramanick

Exam Roll Number : M4CIV1604

Thesis Title : **PULL OUT BEHAVIOUR OF STRIP PLATE ANCHORS IN CLAY BY NUMERICAL MODELLING**

Signature with Date:

JADAVPUR UNIVERSITY
FACULTY OF ENGINEERING & TECHNOLOGY
KOLKATA – 700 032

CERTIFICATE OF RECOMMENDATION

I hereby recommended that the thesis prepared under my supervision by Sri Prasun Chandra Pramanick entitled "**PULL OUT BEHAVIOUR OF STRIP PLATE ANCHORS IN CLAY BY NUMERICAL MODELLING**" be accepted in partial fulfillment of the requirements for the Degree of Master of Civil Engineering with specialization in Soil Mechanics & Foundation Engineering from Jadavpur University

_____

(Dr. Sibapriya Mukherjee)
Professor
Department of Civil Engineering
Faculty of Engineering & Technology
Jadavpur University
Kolkata – 700 032

COUNTERSIGNED BY

_____

Head Of the Department
Department of Civil Engineering
Faculty of Engineering & Technology
Jadavpur University
Kolkata – 700 032

_____

Dean,
Faculty of Engineering & Technology
Jadavpur University
Kolkata – 700 032

JADAVPUR UNIVERSITY
FACULTY OF ENGINEERING & TECHNOLOGY
DEPARTMENT OF CIVIL ENGINEERING
KOLKATA – 700 032

CERTIFICATE OF APPROVAL

This thesis is hereby approved as a creditable study of an engineering subject carried out and presented in a manner satisfactory to warrant its acceptance as a pre-requisite to the degree for which it has been submitted. It is understood that by this approval the undersigned don not necessary endorse or approve any statement made, opinion expressed or conclusion drawn therein, but approve the thesis only for the purpose for which it is submitted.

Board of thesis paper Examiners:

1. _____

2. _____

(Signature of Examiners)

*Only in case the thesis is approved.

ACKNOWLEDGEMENT

The author takes the opportunity to express deep sense of indebtedness to Prof. (Dr.) Sibapriya Mukherjee, Civil Engineering Department (Jadavpur University) for his untiring effort throughout the work by meticulous guidance both during investigation and presentation on this work.

The author must be failing in his duty if he forgets to acknowledge with regards the valuable suggestions and critical comments by Prof. R.B. Sahu, Head of the department of civil Engineering, Jadavpur University.

The author also his conveys heartfelt thanks to Ex. Prof. Shankar Chakroborty (Civil Engineering Dept., Jadavpur University), Prof. G. Bhandari (Civil Engineering Dept., Jadavpur University), Prof. S. Ghosh (Civil Engineering Dept., Jadavpur University), Prof. S.K. Biswas (Civil Engineering Dept., Jadavpur University), Prof. P. Aitch (Civil Engineering Dept., Jadavpur University) for their suggestion, encouragement and hearting support.

Last but not the least my classmates of PG – 2nd Year (2014-16), Geotechnical Engineering Section, Jadavpur University also deserve a special mention.

(Prasun Chandra Pramanick)
Reg. No. – 128863 of 14 – 15
Exam Roll No – M4CIV1604

Department of Civil Engineering
Jadavpur University,
Kolkata – 700032 :

DATED :

LOCATION: Kolkata

ABSTRACT

Soil anchors are commonly adopted as foundation system for structures that require uplift or lateral resistance. For different civil engineering structures like retaining wall, transmission towers etc. anchors are extensively used. Different types of anchors are being employed in the field depending on the magnitude and type of loading, type of structure, importance of the structure and subsoil condition. In the present investigation pull out behavior of strip plate anchors embedded in soft cohesive soil has been studied using a two dimensional finite element model with ABAQUS software. Plate sizes of 50mm, 75mm, and 100 mm with embedment ratios of 1, 2 and 3 have been modelled numerically. A parametric study has been carried out to examine the influence of plate size and embedment ratio on ultimate pull out capacity of plate strip anchors. Further the stress contour for each case has been obtained from the output of the software. They have been studied to understand the change of maximum stress in soil with change of embedment ratio. It has been observed from the study that the ultimate pull out capacity increases with increase of plate size. It has been further observed that maximum stress in soil increases with increase of embedment ratio. The investigation highlights the behavior of strip anchors in respect of variation of ultimate pull out capacity and maximum stress in soil with embedment ratio.

CONTENTS

LIST OF FIGURES

LIST OF TABLES

Chapter – 1

INTRODUCTION

The design of many engineering structures requires that foundation systems resist vertical uplift forces. While mooring structures, offshore platforms, jetty structure and transmission tower are clear examples of structures subjected to uplift. Few structure like building and chimneys are experience pullout loads due to external moment that comes into play.

When pull is applied to an anchor it tries to separate itself from the surrounding soil with the forming of failure surface around the anchor. The shape and extent of failure surface depends on a size and depth of embedment of anchor, evidently depends on the shear strength of soil medium.

The following forces are likely to developed during uplift of an anchor (fig.1.1)

a) Self weight of anchors

b) Weight of soil contained within the failure surface

c) Shear stress developed along the failure surface

d) Reactive forces from the soil remaining unaffected beyond the failure surface.

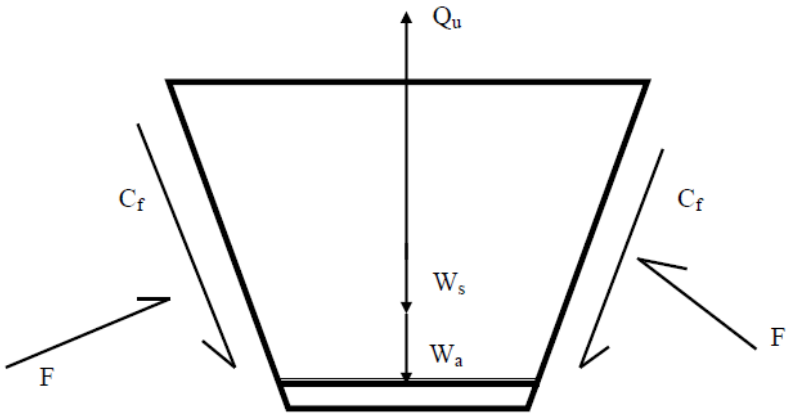

Fig.1.1 Forces developed during pull out of an anchor

W_s = Weight of failure surface of soil

W_a = Self weight of anchor

C_f = Shear stress developed along the failure surface

F = Reactive force from the soil beyond the failure surface

Q_u = Uplift force on the anchor

Different types of anchors are being employed in the field depending on the magnitude and type of loading, type of structure to be supported, importance of the structures and subsoil conditions.

Ultimate resistance of such plate anchors depend on the shape and size of anchor, depth of embedment and characteristics of the embedding soil.

However, only a few research works have been reported so far on the finite element analysis on the behaviour of anchors embedded in clayey soil.

In the present investigation, an attempt has been made to study the ultimate pullout capacity of anchors placed within in embedded soft clay by finite element method using ABAQUS software. The present investigation has been model with variation of embedment depth of anchor and its size. Curves have also been presented showing their variation with embedment ratio and size of anchor.

Further attempt has been made to study the stress contours from the output of ABAQUS and its variation with embedment ratio and plate size.

It has been observed that ultimate pullout capacity and maximum stress contour increases with plate size and embedment ratio.

Chapter – 2

LITERATURE REVIEW

2.1 General:

Different attempt have been made by investigator to study the behaviour of plate anchor and piles subject to different loadings, e.g, vertical, inclined and lateral pulling loads. Experiment were carried out in different soil medium e.g. with cohesive and noncohesive soil; with geotextile and without geotextile.

2.2 Review of Past work:

Meyerhof and Adams (1968) reported that the earlier uplift theories were generally based on either a slip surface rising vertically from the edge of the footing or a surface rising at 30˚ from the vertical forming a frustum. They referred to the work of ***Turner (1962)***, who concluded that the shape of the failure surface had varied with footing dimensions and soil strength and noted a distinct difference in behaviour of shallow and deep footings. They further reported the work of a ***Balla (1961)*** who showed that in dense sand the failure surface for shallow footing was approximately circular in elevation and the tangent to the surface of the ground contact was at an angle of approximately (45˚– ø/2) to the horizontal. Assuming a circular failure path he obtained a reasonable correlation between theory and the result of full-scale tests on shallow footing. Using model tests on sand, ***Macdonald (1963)*** showed that for shallow depths the failure surface was approximately parabolic and for greater depths the failure plane was approximately vertical, the diameter of the cylinder formed being about 1.75 times the base diameter of footing. Macdonald developed two theories to account approximately for this behaviour.

For Shallow case, failure was assumed to be conical, with angle of inclination equal to one half the angle of internal friction. For deep case the failure surface was assumed to be cylindrical with a cylinder diameter of 1.75 times the base diameter. The result of the model tests were reasonable agreement with this theory. Similar tests carried out by Adams and Hayes (1967) and Macdonald (1963) with well graded and uniformly graded sand revealed that in dense sand the uplift capacity increased geometrically with depth.

In loose sand the increase in uplift capacity with depth was approximately linear and much less than in the dense material. The behaviour of both dense and loose uniform sand was observed in semi spatial using time exposure photographs. In the dense sand a shallow depth a distinct slip surface occurred extending in a shallow arc from the anchor surface. At greater depth the failure surface was less distinct being initially curved and then essentially vertical and limited to a short distance above the anchor. In loose sand at shallow depth the failure surface was again essentially vertical but extending to the ground surface. The author (Meyerhof and Adams) further referred to the rest carried out on groups of model footings in sand by **Wiseman** (1966). From the test results, it was observed that for close spacing the failure surface was curved at the outside of the footing and that the soil between the footing moved upward with the footings. Based on the above observation and test data Meyerhof and adams presented an approximate general theory for uplift capacity of a continuous strip footing (Fig.2.1). Because of the complex form of failure surface, Simplifying assumptions in respect of actual failure surface were made by the authors. According to Meyerhof and Adams, the ultimate load per unit length of footing was expressed as:

$$Q_u = 2C_f \cos \alpha + 2F \cos \beta + W \qquad \text{……..…..} (2.1)$$

Where W = Weight of lifted soil mass and weigh of the footing

α and β are average inclination with vertical of forces C_f and F.

C_f = Shear stress developed along the failure surface

F = Reactive force from the soil beyond the failure surface.

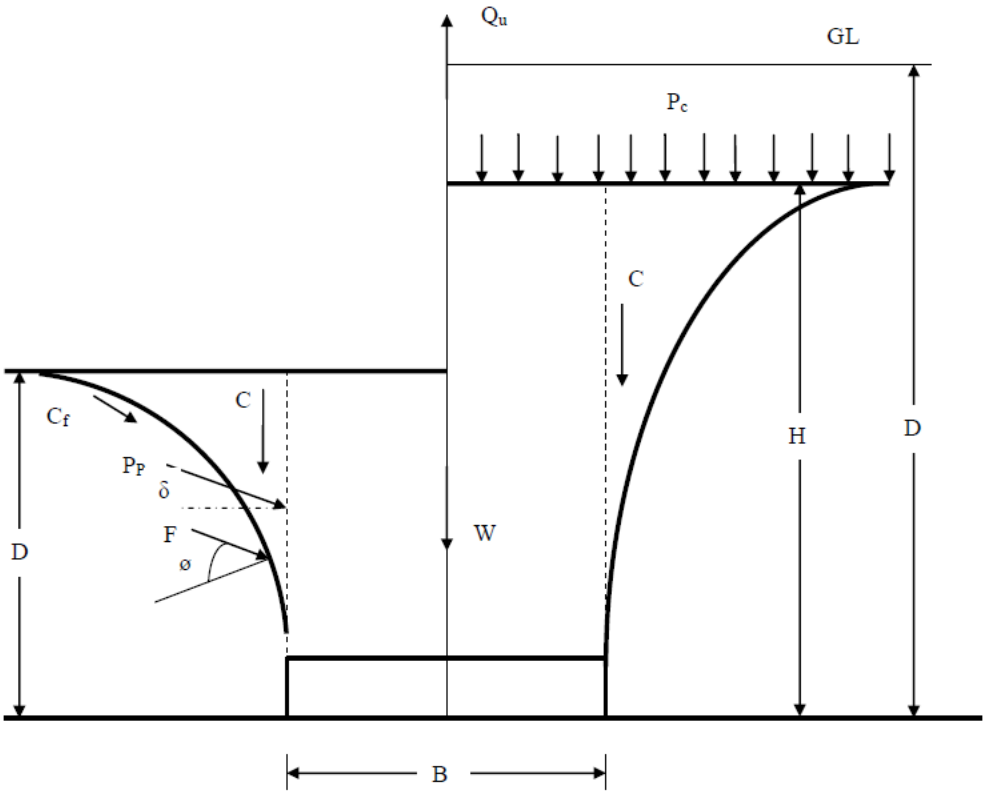

Fig.2.1 Failure of soil above a strip footing under uplift load
by Meyerhof and Adams, 1968

In the absence of a rigorous solution for stresses on the failure surface that Q_U was approximately given by,

$$Q_U = 2\,C + 2\,P_P \sin\delta + W \qquad \text{…….…... (2.2)}$$

Where, C = c. D = Cohesion along vertical plane through footing edge

P_P = Total Passive earth pressure inclined at average angle σ acting downward on vertical plane through footing edge.

Expressing the normal component of P_P ,

$$P_P \cos\delta = K_P\,\gamma\,D^2/2 \qquad \text{…….. (2.3)}$$

K_P = Coefficient of passive earth pressure

γ = Unit of soil and substituting into equation

$Q_U = 2\ C + \gamma D^2\ K_{Pv} + W$ …….. (2.4)

Where, $K_{PV} = K_U \tan \phi = K_P \tan \delta$

K_U = Nominal Uplift coefficient of earth pressure on vertical plane through footing edge

Thus equation becomes,

$Q_U = 2\ C + \gamma D^2\ .K_U \tan \phi + W$ …….. (2.5)

The theory was simplified by considering the forces acting on a cylindrical surface above the foundation. The observed theory was modified to take into account the effect of above group action of square or rectangular footing were sensibly independent of friction angle of sand and embedment depth to width ratio. They also found that uplift coefficient for loose materials were very low and generally about unity. In the absence of full scale tests on footing groups, they examined the result of uplift test on small group of circular shafts. They found that for given density of sand the uplift coefficient of the groups increased roughly linearly with spacing of the footing or shaft and the efficiencies increased as the depth of embedment became smaller. The uplift efficiencies decreased as the number of footings or shafts increased and as the density of sand increased.

Comparison between theory and test result showed better agreement at great depths than at shallow depths, where the estimates were rather conservative. The authors also extended the study for clayey soil and found that drained or long term uplift capacity was appreciably less than the undrained capacity. The reduction with time was attributed to the dissipation of negative pore water pressure which allowed softening of soil. They considered the uplift capacity of soil under purely vertical loading throughout the study.

Chattopadhyay B.C *et. al.* (1986) proposed an analytical method to predict the ultimate uplift capacity of piles embedded in sand. In derivation of net uplift capacity of vertical piles in sand by their proposed theory, they considered the necessary parameter to be angle at shearing resistance (ø) of soil and the pile friction angle (δ). In proposing the theory, they assumed the failure surface to be curved and passing through the soil mass.

The lateral horizontal extent of the failure surface was dependent on the angle of shearing resistance of the surrounding soil, pile friction angle δ and the slenderness ratio S = L/D. The analysis of the results of model piles of themselves and others (Chowdhury & Symons 1983; Das 1983) as well as on driven showed encouraging result and revealed that the theory had potential to predict the ultimate uplift resistance of piles reasonably well. They stated that depending on the reliability of soil data, subsurface information, changes in soil properties for installation etc.

Hanna (1972) identified some of the factors affecting the behaviour of anchors and groups of anchors in sand. Hana provided a practical method of measuring sand movement pattern in the vicinity of the anchors. When a sand surface is loaded by known intensity and then overconsolidation the sand, it was found that, the shape of uplift overconsolidation ratio, the dept of anchor embedment is being constant.

The author carried out experiments prestressed anchors, which were preloaded to a value up to the theoretical design load. After the prestressing phase, the anchor was subsequently loaded to failure through application of external load.

When it was tested to failure, all of the recorded displacements were in an essentially upward direction. The higher the value of initial prestress load value P, the smaller are the movements corresponding to failure.

The behaviour of groups of anchors (not prestressed) were also studied. The anchors used were plate shaped of 38mm diameter and supported by 6mm diameter shaft. It was reported that

increase in depth of embedment from 6 times to 12 times the anchor diameter resulted in an efficiency increase. It was noted, that outer anchors at close spacing but with increase of spacing, all anchors tended to carry equal loads.

At all spacing, the center anchor carried the smallest load, the middle anchors carried intermediate loads. And the corner anchor the targets loads. In groups, anchors interacted and ultimate group efficiencies were less than 100% for the range of depths tested. The author proposed to investigate the following effects for further study.

a) The effect of depth on prestressed anchor behaviour.

b) The effect of repetitive loading on anchor and group of anchors.

c) The behaviour of group of prestressed anchors.

d) The behaviour of group of anchors at very small and very large embedment depth to anchor diameter ratio.

Das (1978, 1980) provided tentative procedures, based on model laboratory tests, for the estimation of the ultimate uplift response of the square anchor plates embedded horizontally in purely cohesive soil. These tests were mostly performed in soft clays and only a limited number of tests were performed in hard clays. The model for the anchor plates employed was 38-50 mm wide and 38-190mm long, and it was vented at the base to eliminate the suction effects by the insertion of a hollow tube. Das provided tentative procedures, based on the model for the laboratory tests, for the estimation of the ultimate uplift response of the square anchor plates embedded horizontally in cohesive soil. These tests were mostly performed in soft clays, but a limited number of tests performed in hard clays. The anchor plate models used had widths of 38 mm - 50 mm and lengths of 38 mm - 190 mm were lidded at the base, in order to eliminate the suction effects by the insertion of a hollow tube. The results showed that the break-out

factor of the foundations located at a relatively shallow depth, increases linearly with the embedment ratio up to a value of about 6. Beyond this value, there was a gradual decrease, reaching a maximum at the critical embedment ratio. The maximum break-out factor was found to be about 9 for the deep soil anchors. Based on the experimental data, Das (1978) suggested procedures to estimate the ultimate uplift response of anchor plates in the cohesive soils.

Das (1978) conducted a number of laboratory tests on the models of the square anchor plates, embedded in the saturated clay with the undrained cohesion (c_u) varying from 5.18 kPa to 172.5 kPa. It was found that the critical embedment ratio $(D/B)_{cr}$ was a function of c_u. The following empirical equations were proposed for the critical embedment ratio.

For square anchor plates

$$(D/B)_{cr-s} = (0.107\ cu + 2.5) \leq 7 \quad \ldots\ldots\ldots\ldots\ldots\ldots (2.6)$$

where

$(D/B)_{cr-s}$ = critical embedment ratio of square or circular plate anchors,

Cu = undrained cohesion in kPa

Rowe *et. al.* (1982) reported results from two dimensional finite element analysis of continuous vertical and horizontal plate anchors. Behaviour of plate anchors in relation to embedment ratio, friction angle, angle of dilatancy, initial stress state, anchor roughness and the orientation of the anchor were examined. It was observed that anchors with horizontal axis exhibited higher collapse load than vertical anchors for similar conditions. Soil dilatancy was found to have a significant effect on the pull out capacity of both types of anchors.

Swamisaran & Rao (2002) studied the behaviour of horizontal plate anchors in cohesionless soil with or without geo-synthetics. Laboratory model tests were performed on square and circular anchors of 100 m width/diameter for embedment depth ratios varying between 2 and 4.2 with single and double layer of geo-grid of size 3 times that of anchor. Placements of geogrids were varied from the top of anchor plate at 0.25 to 0.5 times the depth

of embedment. Based on the experimental results they concluded that inclusion of geo-synthetics increased the pullout capacity significantly and this capacity was found to be dependant on the position of placement of reinforcement above the top of anchor plate which decreased as the distance of the reinforcement from the top of plate increased. Pullout resistance was also found to increase with sand density, depth of embedment and the number of reinforcing layers adopted in the experiment.

Merifield et. al. (2003) estimated the ultimate pullout capacity of different shapes of anchors in clay by using a newly developed three dimensional numerical procedure based on a finite element formulation of the lower bound theorem of limit analysis. From the analysis lower bound estimate of the anchor breakout factor (N_c) was obtained for square, circular and rectangular anchors as shown in Fig.2.2 (a, b & c). Estimated capacities were found to be encouraging while comparing with the available published laboratory model test results. Similar to Merifield (2001), for strip anchors, the anchor capacity was found to increase with overburden pressure upto a limiting value which reflect the transition from shallow to deep anchor behaviour. Moreover according to them, at a given embedment depth an anchor may behave as shallow or deep, depending on the dimensionless overburden ratio $\gamma H/C_u$. From their analysis simple parametric equations for breakout factors as shown below were suggested to find out the capacity of square and circular anchors in homogenous soil profile for different embedment depths.

$$N_{co} = S\,[2.56 \ln (2H/B)] \qquad \ldots\ldots\ldots (2.7)$$

where N_{co} = breakout factor

S = shape factor for square or circular anchor

H/B = embedment ratio

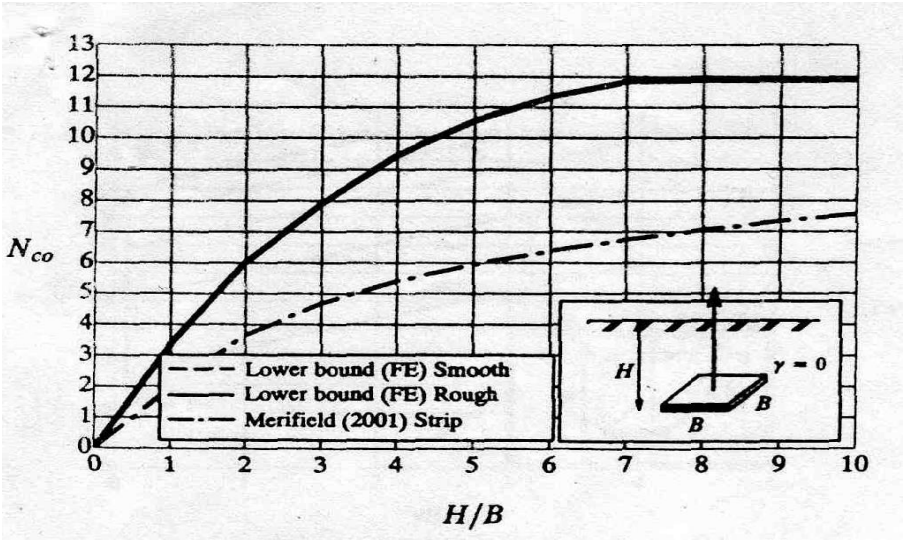

Fig. 2.2(a) Breakout factor for square anchor in clay by Merifield et al, 2003

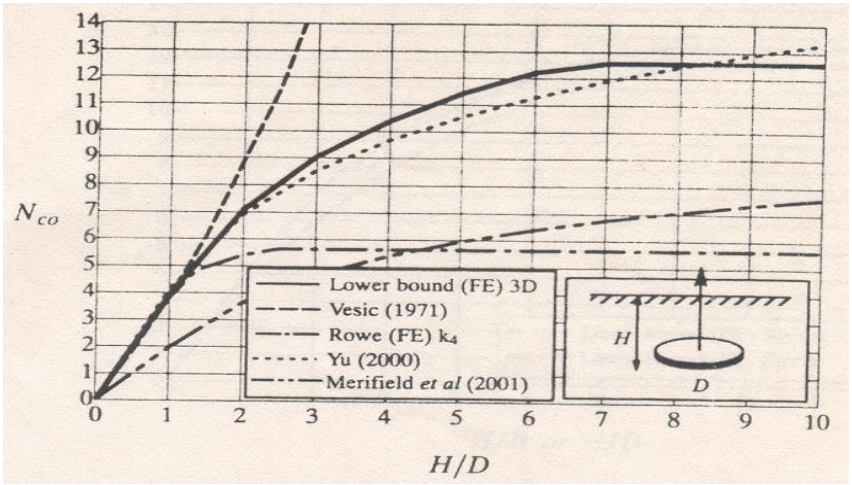

Fig. 2.2(b) Break-out factors for circular anchors in clay by Merifield et al, 2003

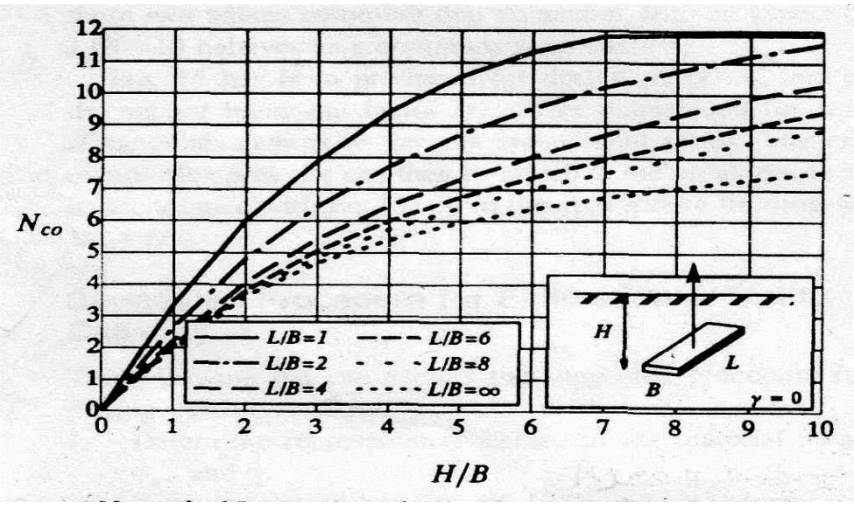

Fig. 2.2(c) Break-out factor for rectangular anchor in clay (Merifield et al, 2003)

Merifield & Sloan (2006) Presented a rigorous numerical analysis to estimate the ultimate pullout capacity for vertical and horizontal anchors in frictional soil. Rigorous lower and upper bound solutions were presented for the ultimate capacity of horizontal and vertical strip anchors in sand. Results were compared with anchor breakout factors estimates obtained using an advanced displacement finite element formulation as shown in Fig.2.3. They concluded that lower bound, upper bound and displacement finite element estimates for the anchor breakout factors compare favorably over the range of embedment depth and frictional angle of soil. Moreover, according to them, the new theoretical prediction when compared with existing theories and laboratory results, it showed encouraging agreement. From their theoretical analysis they also predicted the failure mode for both vertical and horizontal anchors.

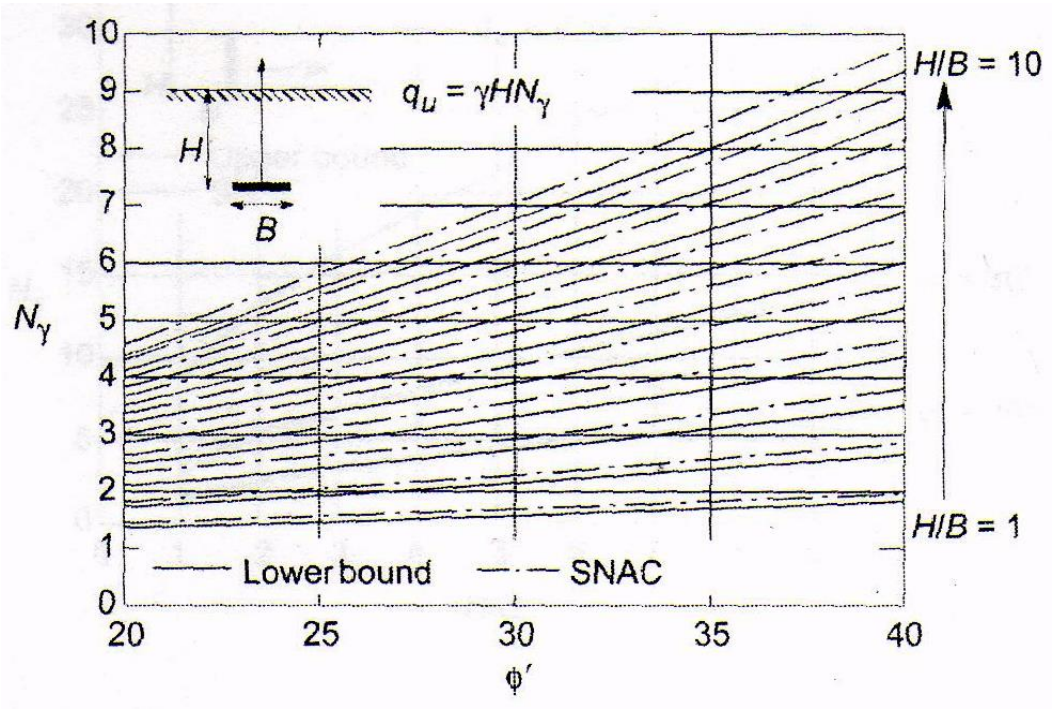

Fig. 2.3 Comparison of break out factors from lower bound limit analysis and solid non-linear analysis by Merifield & Sloan, 2006

Bhattacharya et al. (2008) Studied Behaviour of square plate anchors under uplift load in reinforced clay using a three dimensional finite element displacement model with ANSYS software. Nonlinear soil behaviour with Drucker Prager, the geometrical nonlinearity of geotextile and variable embedment ratio has also been addressed in the analysis. Analysis has been carried out with placement of geotextile varied from the top of the anchor plates. To validate the analysis model tests have also been carried out with 75mm × 75mm and 50mm × 50mm square plates. The results are presented with parametric variation and with normalized plots to obtain an estimate of pullout capacity.

Model tests were conducted to investigate the effect of geosynthetics on load displacement behaviour of square plate anchors of different sizes. All the tests were conducted in a square tank of size 650mm × 650mm and height of 800mm as shown in fig. 2.4. The soil used was dry kaolin which was mixed with requisite amount of water to fill up the test tank up to the required height to obtain different depths of embedment of the anchor plate. The minimum

thickness of the soil cushion was kept at 250mm on which the anchor was placed centrally and before placing the anchor plate

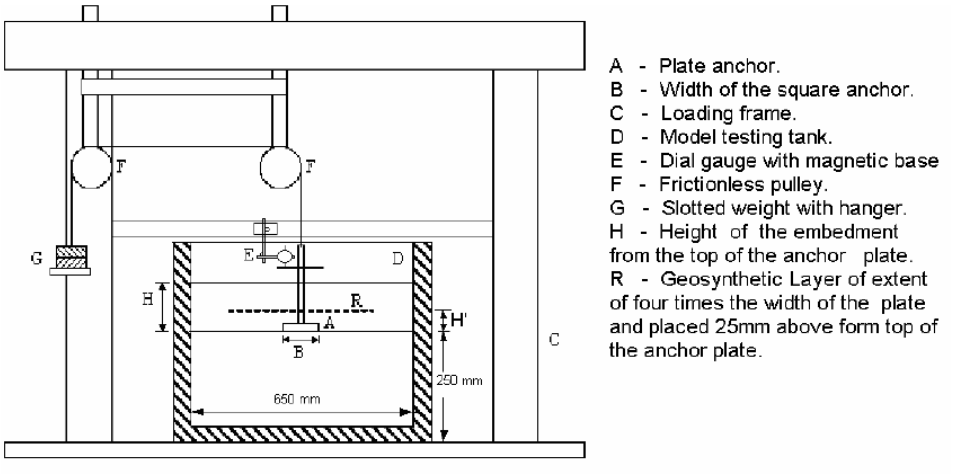

Fig. 2.4. Experimental set up by Bhattacharya et al. (2008)

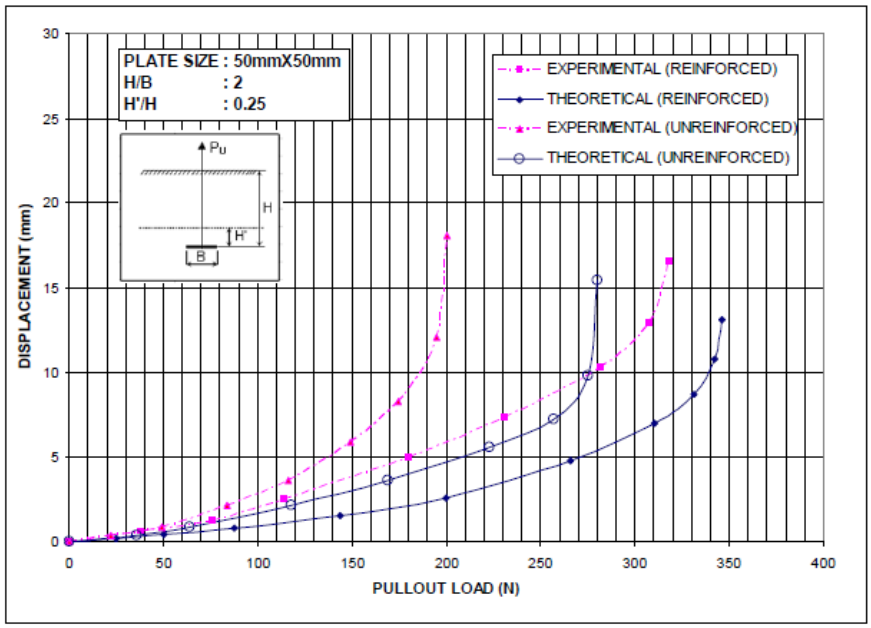

Figure 2.5. Load-Displacement for square anchor plate by Bhattacharya et al. (2008)

In case of reinforced clay, the effect of reinforcement is to mobilize additional shear stress in soils due to appearance of tensile force in the reinforcing material geotextile used in the present

investigation. The breakout factor for reinforced clay has been derived from the ultimate pullout capacity determined from the finite element model and validation of the theory has been carried out by experimental findings for different sizes of square plate anchors in reinforced clay.

The Author noticed so many things on this work, like the ultimate uplift capacity is more in reinforced clay with less ultimate displacement .The uplift capacity is dependent on embedment ratio H/B and the position of the geotextile with respect to the embedment depth. The capacity increases with the increase in embedment ratio but decreases with the increase in height of placement of geotextile above the plate. Maximum value of uplift capacity may be obtained when the geotextile is placed at a depth of 0.25 times the embedment depth and an embedment ratio of 2.0. However beyond an embedment ratio 3, there is marginal increase in the uplift capacity in case of reinforced clay.

Breakout factor for square shallow anchors in reinforced clay has been obtained maximum as 15 which agrees well with the experimental results and also with the available solution by Nene and Garg (1991). However the breakout factor depends on embedment ratio and increases with the increase in embedment ratio up to 4.

Niroumand et al. (2010) studied the ultimate uplift capacity of a horizontal square anchor plate embedded in soft kaolin, loaded here fast enough to be in an undrained condition. The tests were conducted without venting the bottom of the horizontal square anchor plate in order to determine the variation of the embedment ratio. Results are presented in the form of load-displacement curves. The model for the square anchor plate employed a size 50mm. Results showed that the break-out factor of the square anchor plate placed at a relatively shallow depth increases linearly with the embedment ratio up to a value of about 7. The experimental set up is shown in Figures 2.6.

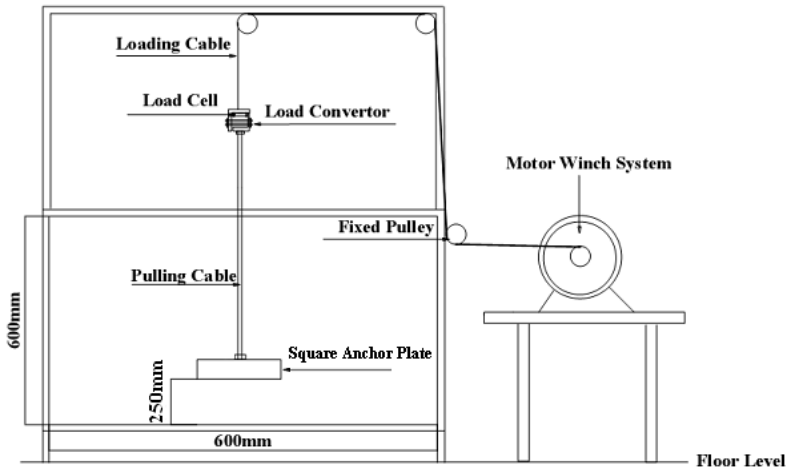

Fig. 2.6. The experimental setup by Niroumand et al. (2009)

Mistri B and Singh B (2011) A parametric study has been carried out to compare the load carrying capacity of rectangular anchor plates for horizontal orientation of the anchor and for varying embedment ratios in soft, medium and stiff clay by finite element modelling using PLAXIS. For the soil, elastic-plastic Mohr-Coulomb model and 15-noded triangular elements are used in the analysis. Mohr Coulomb model has been adopted to predict non-linear behaviour of soil. It involves five input parameters, i.e. E and γ for soil elasticity, $\emptyset$ and c for soil plasticity and ψ for angle of dilatancy. The initial stresses are generated by using Jaky's formula which gives the at rest earth pressure coefficient $K_0 = 1-\sin\emptyset'$, where $\emptyset'$ is termed as angle of internal friction in terms of effective stresses.

The author observed from fig. 2.7 that how shallow and deep plate anchor are classified. If ultimate collapse, the observed failure mechanism reaches the surface then it's classified as shallow. A deep anchor is one whose failure mode is characterized by localized shear around the anchor and is not affected by the location of the soil surface.

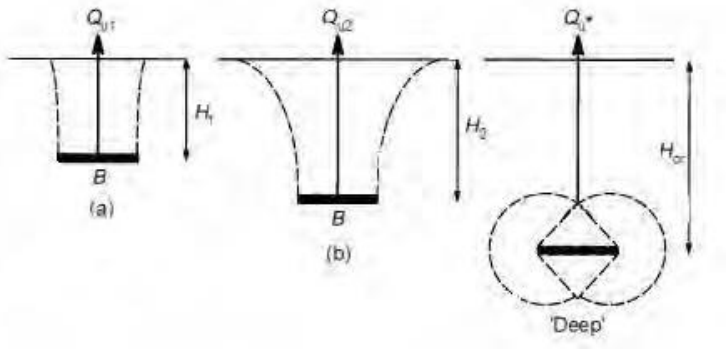

Fig. 2.7 Types of plate anchor based on failure mechanism by Mistri and Singh, 2011

The results obtained are presented in the form of ultimate pullout capacity. The variation in ultimate pullout capacities is in close range for shallow embedment depth. With increase in embedment depth, the variation also increases. Ultimate pullout capacity in homogeneous clay shows a rapid increase initially, after which the rate of increase is less. It may become almost constant at great depth.

Hanna *et. al.* (2014) Carried out an Experimental and analytical investigations on the pull-out capacity of inclined shallow strip plate anchors in sand. A prototype set-up was developed as shown in fig.2.8 to measure the pull-out load and displacement of anchor plates in dense sand. the concept of the plastic limit equilibrium method of analysis was used to develop the analytical model that would utilize the failure mechanism observed during the present experimental investigation. The sand used in the investigation is known commercially as ‘‘Morie Sand’’, which is classified as medium sand with a uniformity coefficient of 1.45. The sand was tested at a relative density of 63.3 %.

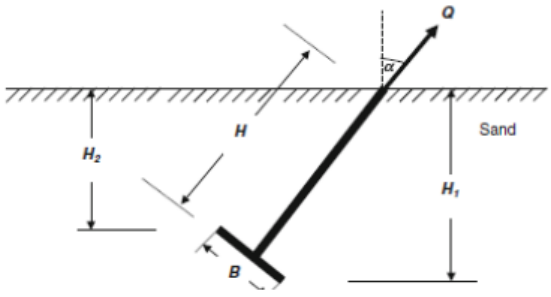

Fig.2.8 Single Plate anchor in sand by Hanna, Foriero and Ayadat (2014)

The Author noticed that the pullout capacity increases with the increase of the inclination angle α of the rod with the vertical, up to a value of 90˚, at which the plate functions as a retaining wall. Furthermore, the pullout capacity Qu increases with the increase of the ratio $\left(\frac{H_1}{B}\right)$ or $\left(\frac{H_2}{B}\right)$ In this investigation, the pullout capacity Qu was determined from the load–displacement curve, The peak value on the curve is the pullout capacity or at the point beyond which displacement continue to increase without increased in the pullout load.

Based on the result of the present experimental investigation, the following relationship was proposed by author:

$$Q_u = 63.\ e^{\,0.1Uf} \qquad \text{.....(2.8)}$$

Q_u = Ultimate pullout capacity

Uf = Displacement at failure

It can be noted as expected that the bottom edge of the plate is always subjected to higher pressure compared to the top edge, and accordingly the failure mechanism starts at the bottom edge of the anchor and propagates upwards until it reaches the ground level. Rupture surface was roughly a truncated conical shape, which is further deflated at an increase in the angle of inclination of the anchor.

Suganya A and Arumairaj P.D (2015) carried out an experimental study on horizontal circular plate anchor of various diameter embedded into cohesion less soil medium (sand). Also varying depth of plate anchor resulting embedment ratio and geogrid diameter with respect to plate diameter.

Experiment is carried out in a model tank. Embedded circular plates were attached to steel wire for pulling it axially in vertical direction. Tamping technique is adopted to achieve uniform sand bed of required density for medium and dense sand conditions. The plate anchors were subjected to increasing pulling loads till failure, accompanied with measurement of vertical movement. Finally finding the break out pulling load for each cases.

Various observation has been shown like the breakout capacity of shallow anchors can be increased many ways by adopting geogrid of suitable diameter depending on the requirement of increase, the pullout capacity increases with increase in diameter of geogrid, embedment ratio

Chapter – 3

OBJECTIVE AND SCOPE

3.1 OBJECTIVE

The principal objective of this work is to study the behaviour of strip plate anchors of different sizes embedded in cohesive soil under the axial vertical pull.

3.2 SCOPE OF WORK

In order to full fill the above object a numerical study has been carried out by Finite Element Method using ABAQUS Software. Total 9 number of numerical cases have been carried out with variation of plate size and embedment depth as follows:

I. Anchor Size : 50mm strip, 75mm strip, 100mm strip

II. Embedment Ratio (H/B) : Ratio of embedment depth of soil to the width of the plate (H/B) are 1, 2 and 3

Chapter – 4

NUMERICAL STUDY

4.1 GENERAL

In the finite element analysis the entire domain has been discretized by 4 noded quadrilateral elements. Soil nonlinearity have been considered. In their present study soil has been idealised as elastic-perfectly plastic material satisfying Mohr-Coulomb criterion.

4.2 Finite Element Formulation

In the present investigation geometry and loading do not vary significantly in the longitudinal direction so plain strain criteria has been adopted. For 4 noded quadrilateral element each node of the element has two degrees of freedom, displacement (u) in the horizontal direction (x) and displacement (v) in the vertical direction (y) as shown in Fig. 4.1.

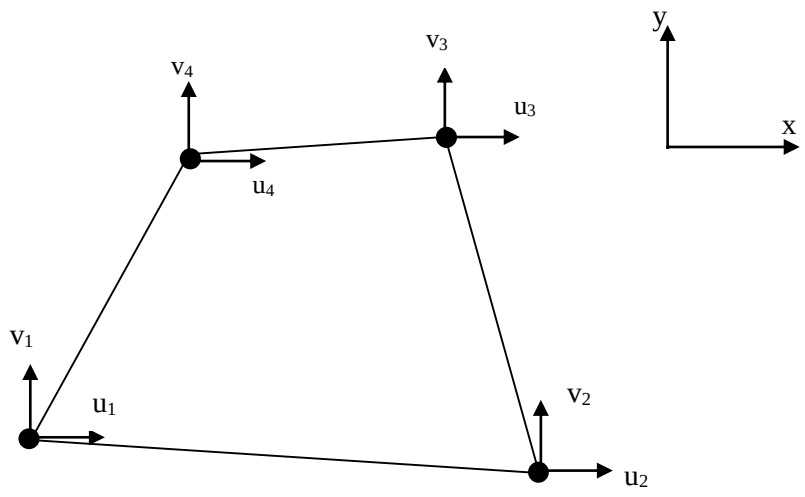

a) Typical Element

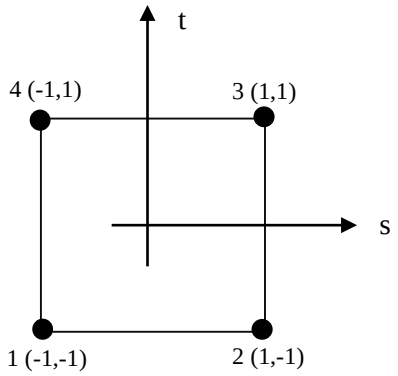

b) parent element

Fig. 4.1 Four-Noded quadrilateral element for plain strain

The generalised displacement vector (u) at a point within an element is related to the nodal displacement vector (q) by shape function matrix [N]

as, $\{u\} = \begin{Bmatrix} u \\ v \end{Bmatrix} = [N]\{q\}$ ..... (4.1)

where {u} =displacement vector at the point within an element,

$\{q\}^T = \{u_1, v_1, u_2, v_2, u_3, v_3, u_4, v_4,\}$ ..... (4.2)

And $[N] = \begin{bmatrix} N_1 & 0 & N_2 & 0 & N_3 & 0 & N_4 & 0 \\ 0 & N_1 & 0 & N_2 & 0 & N_3 & 0 & N_4 \end{bmatrix}$ ..... (4.3)

Shape function for parent element using Lagrange interpolation formula

$N_1 = \frac{1}{4}(1 - s)(1 - t)$ ..... (4.4)

$N_2 = \frac{1}{4}(1 + s)(1 - t)$ ..... (4.5)

$N_3 = \frac{1}{4}(1 + s)(1 + t)$ ..... (4.6)

$N_4 = \frac{1}{4}(1 - s)(1 + t)$ ..... (4.7)

Iso-parametric mapping: interpolate the geometry using shape functions

$x = [N_1 \quad N_2 \quad N_3 \quad N_4] \begin{Bmatrix} x_1 \\ x_2 \\ x_3 \\ x_4 \end{Bmatrix}$ $y = [N_1 \quad N_2 \quad N_3 \quad N_4] \begin{Bmatrix} y_1 \\ y_2 \\ y_3 \\ y_4 \end{Bmatrix}$ ..... (4.8)

The nodal displacements are

$u = \sum_{i=1}^{4} N_i u_i$ …… (4.9)

$v = \sum_{i=1}^{4} N_i v_i$ ……(4.10)

The strain vector, {ε} is expressed in terms of the nodal displacements as given below:

$$\{\epsilon\} = \begin{Bmatrix} \epsilon_x \\ \epsilon_y \\ \tau_{xy} \end{Bmatrix} = \begin{Bmatrix} \delta u/\delta x \\ \delta v/\delta y \\ \delta u/\delta y + \delta v/\delta x \end{Bmatrix} = [B]\{q\} \quad \text{…… (4.11)}$$

where {ε} = strain vector

[B] = strain displacement transformation matrix consisting of derivatives of shape function

i.e. $[B] = [B_1]\,[B_2]$ ……..$[B_4]$

and $[B_i] = \begin{bmatrix} \frac{\delta N_i}{\delta x} & 0 \\ 0 & \frac{\delta N_i}{\delta y} \\ \frac{\delta N_i}{\delta y} & \frac{\delta N_i}{\delta x} \end{bmatrix}$ …… (4.12)

The stress-strain relationship for elastic material is expressed as,

$\{\sigma\} = [D_e]\,\{\varepsilon\}$

Where, $\{\sigma\} = \begin{Bmatrix} \sigma_x \\ \sigma_y \\ \tau_{xy} \end{Bmatrix}$ = stress component vector …… (4.13)

And $[D_e]$ = Elasticity matrix

$$[D_e] = \frac{E}{(1+v)(1-2v)} \begin{bmatrix} 1-v & v & 0 \\ v & 1-v & 0 \\ 0 & 0 & \frac{(1-2v)}{2} \end{bmatrix} \quad \text{…… (4.14)}$$

Where, E = modulus of elasticity, υ being the Poisson's ratio

The shape functions used for describing the geometry of the element and displacement variation are expressed in terms of local coordinates (s,t) and it is required to determine the derivatives of the of the functions with respect to global coordinates (x,y).

From the chain rule of differentiation the relationship between two coordinate system is given below

$$\begin{Bmatrix} \frac{\delta N_i}{\delta x} \\ \frac{\delta N_i}{\delta y} \end{Bmatrix} = [J]^{-1} \begin{Bmatrix} \frac{\delta N_i}{\delta s} \\ \frac{\delta N_i}{\delta t} \end{Bmatrix} \quad \ldots\ldots\ldots\ldots (4.15)$$

Where [J] is known as the Jacobian Matrix

$$J = \begin{bmatrix} \frac{\delta x}{\delta s} & \frac{\delta y}{\delta s} \\ \frac{\delta x}{\delta t} & \frac{\delta y}{\delta t} \end{bmatrix} \quad \ldots\ldots\ldots (4.16)$$

And $[J]^{-1}$ is the inverse of the Jacobian Matrix.

The variation function for the displacement method is given by the potential energy π_p of the system and it can be expressed as

$$\pi_p = \int v dU(u,v) dV - \int v(Ru + Zv) dV \quad \ldots\ldots\ldots\ldots (4.17)$$

dU (u,v) = Strain energy per unit volume

R, Z = Components of body forces

V = Volume of the element

Now for static equilibrium of a system, condition of minimum potential energy is to apply which yields:

$$\delta(\pi_p)/\delta q = 0 \quad \ldots\ldots\ldots\ldots (4.18)$$

$$\delta(\pi_p)/\delta q = \int_V [B]^T [D_e][B]\{q\} dv - \int_V [N]^T \{R\} dv = 0 \quad \ldots\ldots\ldots\ldots (4.19)$$

$$\int_V [B]^T [D_e][B]\{q\} dv = \int_V [N]^T \{R\} dv \quad \ldots\ldots\ldots (4.20)$$

$$[K]\{q\} = \{Q\} \quad \ldots\ldots\ldots (4.21)$$

Where, Element stiffness matrix [K] is given by

$[K] = \int_V [B]^T [D_e][B] dV$ …… (4.22)

$\{Q\} = \int_V [N]^T \{R\} dv = \text{nodal load vector}$ …… (4.23)

In global relationship the stiffness matrix [K] for the entire system is given

by $[K]\{\delta\} = \{F_s\}$ ……....(4.24)

where,

[K] = Global stiffness matrix

{δ}= Global nodal displacement vector

$\{F_S\}$= Global nodal force vector.

The global stiffness matrix is obtained by adding for approximately the individual contributions from elements which are common to node.

4.3 Material nonlinearity

At higher stress level, the stress-strain characteristic of soil becomes nonlinear. Therefore, soil has been idealised as an elastic-perfectly plastic material satisfying Mohr-Coulomb yield criterion. Mohr-Coulomb model requires a total of five parameters, which are generally familiar to most geotechnical engineers and which can be obtained from basic tests on soil samples. These parameters with their standard units are listed below.

E =Young's Modulus (kN/m^2); υ= Poisson's Ratio; ψ = Dilatancy angle; c = cohesion;

Ø = Friction angle.

It is quite generally postulated as an experimental fact that yielding can occur only if stress σ satisfies the general yield criterion:

$F(\sigma, K_h) = 0$ …… (4.25)

Where, K_h = hardening parameter and F is the yield function.

For isotropic cases the yield surface is conveniently expressed in terms of the three stress invariants, i.e,

σ_m= Pure hydrostatic stress = $J_1/3 = \frac{\sigma_x+\sigma_y+\sigma_z}{3}$ …….. (4.26)

However, in this formulation $\sigma_z = 0$, under plane strain condition

$$\sigma = J_2^{1/2} = \left[\frac{1}{2}(S_x^2 + S_y^2 + S_z^2) + \tau_{xy}^2 + \tau_{yz}^2 + \tau_{zx}^2\right]^{\frac{1}{2}} \quad \text{……. (4.27)}$$

A potential surface is defined by $Q = Q(\sigma, k_h)$ which defines the plastic strain increment $d\varepsilon_p$ as $d\varepsilon_p = \lambda \frac{\delta Q}{\delta \sigma}$ …… (4.28)

Where, $\lambda = \left\{\frac{\partial F}{\partial \sigma}\right\}^T [De] \{d\varepsilon\}/\{\delta F/\delta\sigma\}^T[De]\{\delta Q/\delta\sigma\}+A$ …… (4.29)

The particular case of Q = F is known as associated plasticity, otherwise the plasticity follows non-associated flow rule. The elasto plastic matrix $[D_{ep}]$ is derived as

$$[D_{ep}] = [D_e] - [D_e]\left\{\frac{\delta Q}{\delta\sigma}\right\}\left\{\frac{\delta F}{\delta\sigma}\right\}^T [De] \times [A+\left\{\frac{\delta F}{\delta\sigma}\right\}^T [D_e]\left\{\frac{\delta Q}{\delta\sigma}\right\}^{-1} \quad \text{……..(4.30)}$$

For ideal plasticity with no hardening, A becomes equal to zero. The stress increment vector $\{\Delta\sigma\}$ is related to strain increment vector $\{\Delta\varepsilon\}$ as

$\{\Delta\sigma\} = [Dep] \{\Delta\varepsilon\}$ …… (4.31)

Chapter – 5

FINITE ELEMENT ANALYSIS: Modelling by ABAQUS

5.1 General

This chapter presents the background of numerical study carried out using finite element software ABAQUS. The ABAQUS finite element system includes ABAQUS/Standard, a general-purpose finite element program; ABAQUS/Explicit, an explicit dynamics finite element program; ABAQUS/CAE, an interactive environment used to create finite element models, submit ABAQUS analysis, monitor and diagnose jobs, and evaluate results.

5.2 Material model

Predicting soil behaviour by constitutive equation that are based on experimental finding and embodied in numerical method such as the finite element method is a significant aspect of soil mechanics. This finite element method used to solve several of geotechnical engineering problems, especially problems that are complex and cannot be solved using traditional analysis without making simplifying assumption that may jeopardize the value of the analytical solution. Soils are constituted of discrete particles, and most soil models assume that the forces and displacements within this particles are represented by continuous stresses and strains.

Elastic and Elastic-plastic soil model are adopted in this numerical study.

5.2.1 Elastic model

The basic assumption of elastic behaviour, is that the directions of principal incremental stress and incremental strain coincide. The general constitutive matrix relates increments of total stress to increments of strain:

$$\begin{Bmatrix} \Delta\sigma_x \\ \Delta\sigma_y \\ \Delta\sigma_z \\ \Delta\tau_{xz} \\ \Delta\tau_{yz} \\ \Delta\tau_{xy} \end{Bmatrix} = \begin{bmatrix} D_{11} & D_{12} & D_{13} & D_{14} & D_{15} & D_{16} \\ D_{21} & D_{22} & D_{23} & D_{24} & D_{25} & D_{26} \\ D_{31} & D_{32} & D_{33} & D_{34} & D_{35} & D_{36} \\ D_{41} & D_{42} & D_{43} & D_{44} & D_{45} & D_{46} \\ D_{51} & D_{52} & D_{53} & D_{54} & D_{55} & D_{56} \\ D_{61} & D_{62} & D_{63} & D_{64} & D_{65} & D_{66} \end{bmatrix} \begin{Bmatrix} \Delta\varepsilon_x \\ \Delta\varepsilon_y \\ \Delta\varepsilon_z \\ \Delta\gamma_{xz} \\ \Delta\gamma_{yz} \\ \Delta\gamma_{xy} \end{Bmatrix} \quad \text{.....(5.1)}$$

it is possible to divide the total stress constitutive matrix [D], given above, into the sum of the effective stress matrix [D'] and the pore fluid matrix [D_f]. Consequently, the constitutive behaviour can be defined either by [D] or [D'].

In present numerical model linear isotropic elasticity and elasto-plasticity criteria have been adopted.

5.2.1.1 Linear isotropic elasticity

An isotropic material is one that has point symmetry, i.e. every plane in the body is a plane of symmetry for material behaviour. In such a situation it can be shown that only two independent elastic constants are necessary to represent the behaviour and that the constitutive matrix becomes symmetrical. In structural engineering it is common to use Young's modulus, E', and Poisson's ratio, μ', for these parameters. Equation (5.1) then takes the form shown in Equation (5.2). If the material behaviour is linear then E' and μ' are constants and the constitutive matrix expressed as a relationship between accumulated effective stresses {σ') and strains {ε} is the same as that given in Equation (5.2). It is also possible to express the constitutive matrix as a relationship between total stress and strain, either on an incremental or

accumulated basis. In this case the appropriate parameters are the undrained Young's modulus, E_u, and Poisson's ratio, μ_u.

$$\begin{Bmatrix} \Delta\sigma'_x \\ \Delta\sigma'_y \\ \Delta\sigma'_z \\ \Delta\tau_{xz} \\ \Delta\tau_{yz} \\ \Delta\tau_{xy} \end{Bmatrix} = \frac{E'}{(1+\mu')(1-2\mu')} \begin{bmatrix} 1-\mu' & \mu' & \mu' & 0 & 0 & 0 \\ & 1-\mu' & \mu' & 0 & 0 & 0 \\ & & 1-\mu' & 0 & 0 & 0 \\ & & & \frac{1-2\mu'}{2} & 0 & 0 \\ & sym & & & \frac{1-2\mu'}{2} & 0 \\ & & & & & \frac{1-2\mu'}{2} \end{bmatrix} \begin{Bmatrix} \Delta\varepsilon_x \\ \Delta\varepsilon_y \\ \Delta\varepsilon_z \\ \Delta\gamma_{xz} \\ \Delta\gamma_{yz} \\ \Delta\gamma_{xy} \end{Bmatrix} \quad \ldots\ldots(5.2)$$

For geotechnical purposes, it is often more convenient to characterize soil behaviour in terms of the elastic shear modulus, G, and effective bulk modulus, K'. Equation (5.1) then becomes:

$$\begin{Bmatrix} \Delta\sigma'_x \\ \Delta\sigma'_y \\ \Delta\sigma'_z \\ \Delta\tau_{xz} \\ \Delta\tau_{yz} \\ \Delta\tau_{xy} \end{Bmatrix} = \begin{bmatrix} K'+\frac{4}{3}G & K'-\frac{2}{3}G & K'-\frac{2}{3}G & 0 & 0 & 0 \\ & K'+\frac{4}{3}G & K'-\frac{2}{3}G & 0 & 0 & 0 \\ & & K'+\frac{4}{3}G & 0 & 0 & 0 \\ & & & G & 0 & 0 \\ & sym & & & G & 0 \\ & & & & & G \end{bmatrix} \begin{Bmatrix} \Delta\varepsilon_x \\ \Delta\varepsilon_y \\ \Delta\varepsilon_z \\ \Delta\gamma_{xz} \\ \Delta\gamma_{yz} \\ \Delta\gamma_{xy} \end{Bmatrix} \quad \ldots\ldots\ldots\ldots\ldots(5.3)$$

Where

$$G = \frac{E'}{2(1+\mu')} \quad ; \quad K' = \frac{E'}{3(1-2\mu')} \qquad \ldots\ldots\ldots(5.4)$$

It is also possible to express the constitutive matrix in terms of undrained stress parameters. As water cannot sustain shear stresses, the undrained and effective shear modulus are the same, hence the use of G without a prime in Equations (5.3) and (5.4). Consequently, only K' has to be replaced by K_u in Equation (5.4) to obtain the total stress constitutive matrix, [D].

5.2.2 Elasto-plastic behaviour Model

Elastic constitutive models are relatively simple, they cannot simulate many of the important characteristics of real soil behaviour. Improvements can be made by extending these models using the theory of plasticity. Elasto-plastic behaviour Model Mohr-coulomb is presented below

5.2.2.1 Mohr-coulomb model

The characteristics of the Mohr-Coulomb plasticity model in ABAQUS:

- The model is intended for granular materials like soils under monotonic loading.
- It does not consider rate dependence.
- The linear isotropic elastic response is followed by non-recoverable response idealized as being plastic.
- The yield behaviour depends on the hydrostatic pressure:
- The material becomes stronger as the confining pressure increases.
- The yield behaviour may be influenced by the magnitude of the intermediate principal stress.
- The model includes isotropic hardening or softening.
- The inelastic behaviour is generally accompanied by volume change.
- The flow rule may include:
    - Inelastic dilation as well as
    - Inelastic shearing
- The plastic flow potential is smooth and non-associated.
- Material properties can be temperature dependent.
- Tension cutoff can be used to limit the tensile strength.

The Mohr-coulomb model is intended for granular material like soil, the linear isotropic response is followed by non-recoverable response idealized as plastic behaviour, yield behaviour is depend on the hydrostatic pressure, provided isotropic hardening and softening. The Mohr-Coulomb failure or strength criterion has been used for geotechnical applications. A large number of the routine design calculations in the geotechnical area are still performed using the Mohr-Coulomb criterion.

The model isotropic elasticity and the yield function is given by

$$F = R_{mc}q - p\tan\phi - c = 0, \qquad \text{……(5.5)}$$

Where, $R_{mc}(\Theta,\phi)$ is a measure of the shape of the yield surface in the deviatoric plane

$$R_{mc} = \frac{1}{\sqrt{3}\cos\phi}\sin\left(\Theta+\frac{\pi}{3}\right)+\frac{1}{3}\cos\left(\Theta+\frac{\pi}{3}\right)\tan\phi, \qquad \text{…….(5.6)}$$

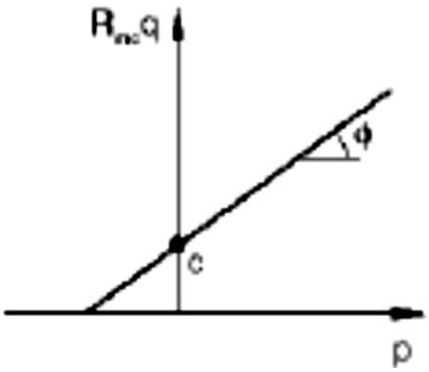

Fig. 5.1 Yield surface in the meridionial plane

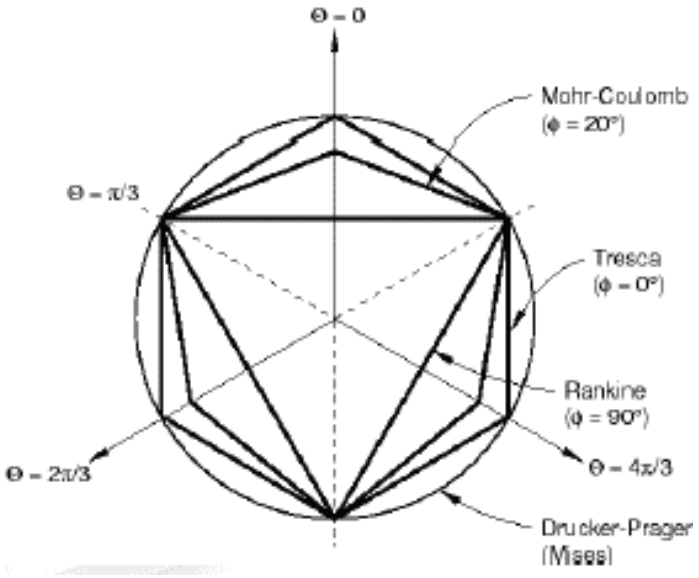

Fig. 5.2 Yield surface in the deviatoric plane

From fig. 5.1 ϕ is the slope of the Mohr-Coulomb yield surface in the $R_{mc}q - p$ stress plane, which is commonly referred to as the friction angle of the material, c is the cohesion of the material; and Θ is the deviatoric polar angle defined as

$$\cos(3\Theta) = \frac{r^3}{q^3} \qquad \text{……..(5.7)}$$

The Mohr- coulomb model is assumed that the hardening is defined by the material cohesion, 'c'. These above model can be employed for the material modelling of plate anchor embedded into the soft soil. The linear elastic can be used for plate anchor and Mohr-coulomb model can be employed for soft soil.

5.3 Numerical modelling in ABAQUS

Soil, is being analysed numerically as plain strain Mohr Coulomb elasto-plastic model in ABAQUS. The Plate anchor is modelled as 2D planer solid homogeneous which is embedded into soft clay medium with various embedded ratios 1, 2 and 3. Following plate anchor size are taken in strip a) 50mm b) 75 mm and c) 100 mm

5.3.1 Geometry

There are two part of modelling i) plate anchor and ii) soil. All are 2D planer shell type. The length (along X-direction) and depth (along Y-direction) of the soil profile is create 10 times of plate size as shown in fig. 5.3 below.

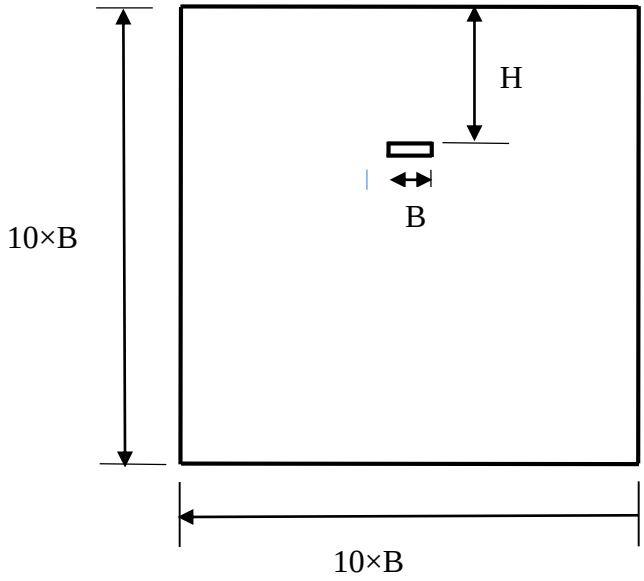

B = width of the plate
H/B = Embedment ratio

Fig. 5.3 Model Sketch in geometry

5.3.2 Boundary Conditions

It is considered that the bottom of the model is fixed that means no displacement and rotation will occur in any direction. That's why at bottom of model assign Encastre type Boundary condition. In vertical edges of model only horizontal displacement is restricted, vertical displacement is allowed to move freely. In this case displacement / Rotation boundary condition is used. And apply adequate displacement to the plate anchor under Displacement/ Rotation boundary condition.

5.3.3 Material Property:

The material properties for plate anchor and soft clay sample are given below in table 5.1 and 5.2

i. **Plate anchor (Material –I) :** Material used in plate anchor is mild steel.

Table 5.1 Properties of Plate Anchor

Sl. No.	Parameter	Value	Unit
1	Mass Density (ρ)	7850	Kg/m^3
Linear Elastic Property			
2	Young Modulus (E)	2×10^{11}	N/m^2
3	Poisson's ratio (μ)	0.33	--

ii. **Soil (Material –II) :** Material type used in soil is soft clay

Table 5.2 Properties of Soil

Sl. No.	Parameter	Value	Unit
1	Mass Density (ρ)	1800	Kg/m^3
Linear Elastic Property			
2	Young Modulus (E)	7500000	N/m^2
3	Poisson's ratio (μ)	0.4	--
Elasto-plastic (Mohr Coulomb) Property			
1	Friction Angle (ø)	7˚	--
2	Dilation Angle (ψ)	0˚	--
3	Cohesion Yield Stress	15000	N/m^2
4	Cohesion Yield Strain	0	--

5.3.4 Interaction Properties

To simulate exact field condition to provide interaction property between the soil layer and between the plate anchors. Surface base contact simulation generally needs to define mechanical contact property models in two directions: normal direction and tangential direction. Here all the interacting surfaces are considered as rough for tangential behaviour. Rough contact property defines the frictional property of the surfaces. The rough behaviour denotes that there is an infinite coefficient of friction between the surfaces and no slip will occur along the surfaces. The sliding along the surfaces is considered as finite sliding. The "hard contact" is assumed in normal direction. Interaction condition applied to the model in ABAQUS environment as shown in fig. 5.4.

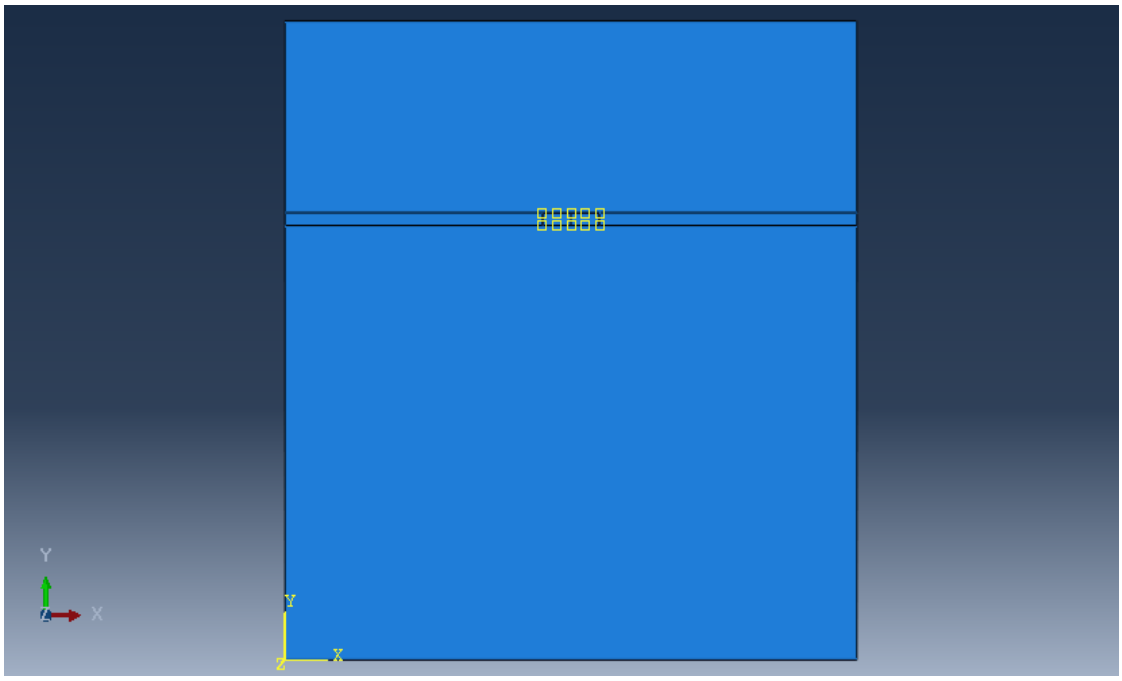

Fig. 5.4 Interaction condition shown in model

5.3.5 Meshing

Meshing criteria is one of the most important features in finite element analysis. The result of analysis can change significantly. ABAQUS offer different type of element such as plane strain element, plane stress element, pore fluid stress element etc. In this analysis plain strain element CPE4R, a 4-node bilinear plane strain quadrilateral element with reduce integration is used.

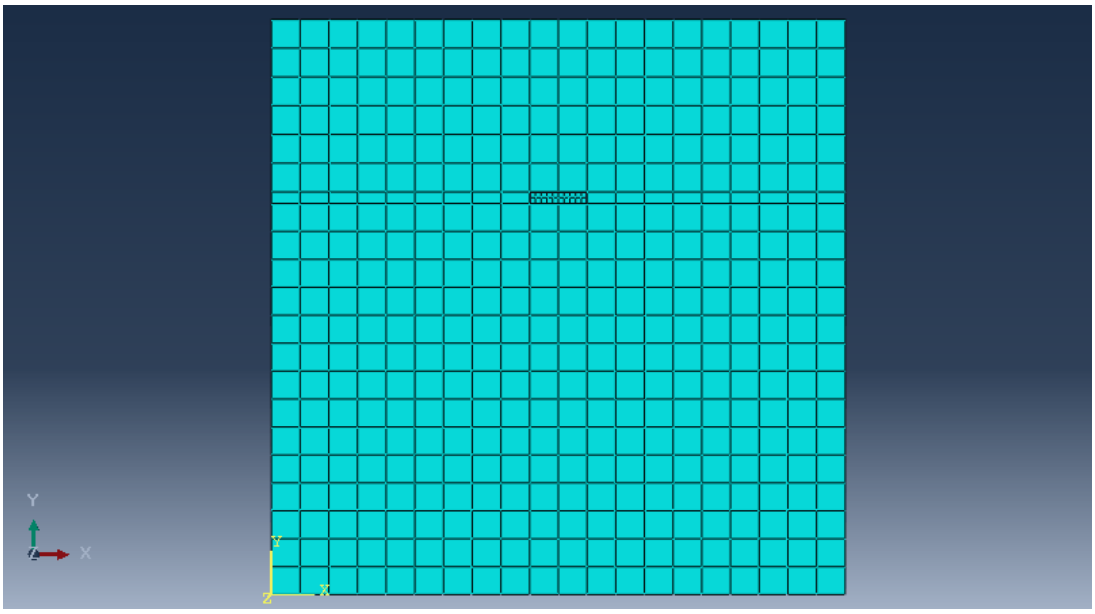

Fig. 5.5 Meshed Part before analysis of model

5.3.6 Application of Displacement

The adequate deformation is applied on plate in static general step. The value of time period for application of deformation given as 10 sec. In this step, the deformation is applied in maximum 100 increments. Here in this step direct method is chosen as equation solver. Use solver default matrix storage and full newton solution technique is chosen.

The finite element model created in ABAQUS CAE environment is submitted for analysis. Data check operation has been carried out before analysis. During data check the ABAQUS

processor show some warning and no error is obtained. The job is submitted for analysis and result are taken. The warning appeared during data check is as follows

i. The dilation angle is small or zero. The value will be set to 0.10000

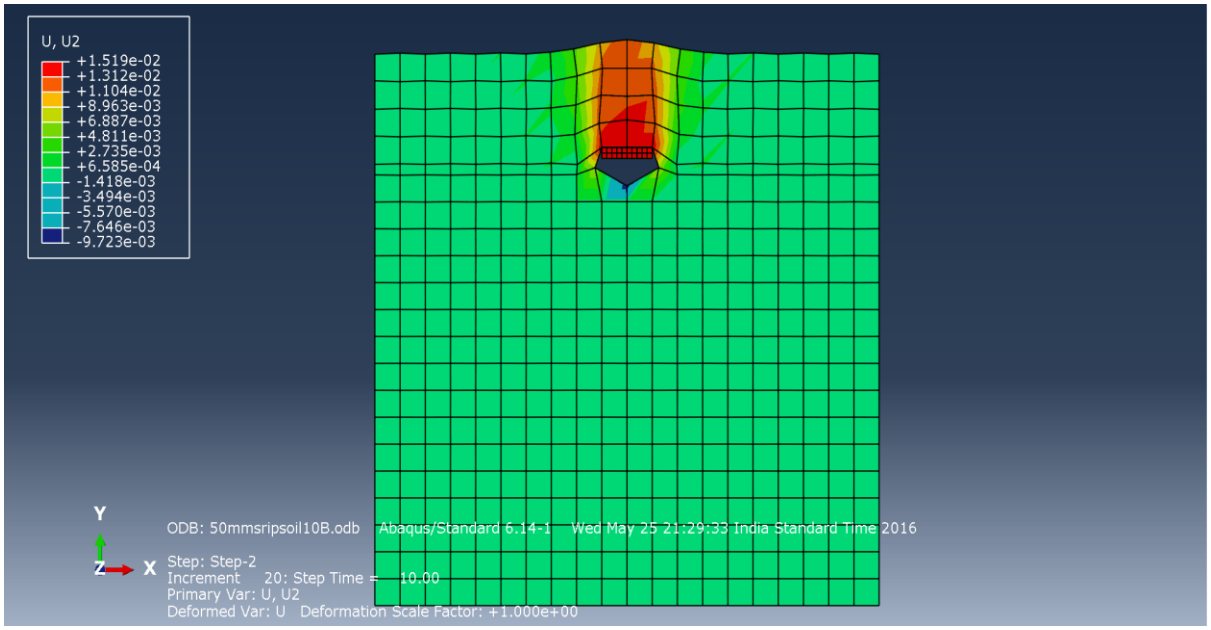

Fig. 5.6 Typical deform shape of 50 mm wide strip
of embedment ratio (H/B) 2

Chapter – 6

RESULTS AND DISCUSSION

6.1 General

In the present study an attempt has been made to carry out numerical analysis of strip plate anchors of sizes 50 mm, 75 mm and 100 mm by finite element method using ABAQUS Software. The output of the software has helped to determine ultimate pull out capacity of the anchors and the corresponding stress contours for different plate sizes with embedment ratio of 1, 2 and 3. In this chapter the numerical results have been presented and an attempt has also been made to make to interpret the results.

6.2 List of Numerical Cases

The cases analysed by numerical techniques have been listed in table 6.1

Table 6.1 List of numerical cases

Sl. No.	Plate Size (B) in mm	Embedment Ratio (H/B)
1	50	1
2		2
3		3
4	75	1
5		2
6		3
7	100	1
8		2
9		3

6.3 Numerical Results

The numerical results have been obtained from the output of ABAQUS in the form of load Vs. displacement curves for all the cases. The stress contours have also been obtained for the nine (9) cases with the help of ABAQUS software. Load vs. Axial displacement curves have been presented for all the cases from fig.6.1 to fig.6.9. The stress contours have also been presented in fig.6.12 to fig.6.20

6.4 Discussion on Results

Based on the numerical results presented in section 6.2 an attempt has been made to study the load displacement curves obtained from numerical analysis. The variation of ultimate pull out capacity with plate size and also with embedment ratio has also been studied. Further attempt has also been made to study the variation of maximum stress in soil with plate size with embedment ratio.

6.4.1 Pull out Load Vs. Axial Displacement Curves

The pull out load vs axial displacement curves for all the cases have been shown in fig 6.1 to fig. 6.9. It appears from the figures that the pull out load vs. axial displacement response is nonlinear up to failure. Axial displacement increases with pull out load in all cases as seen in the figure. The peak loads have been adopted as ultimate pull out capacity for all the cases. The ultimate pullout capacity and axial displacement at failure for all tests are presented in Table. 6.2.

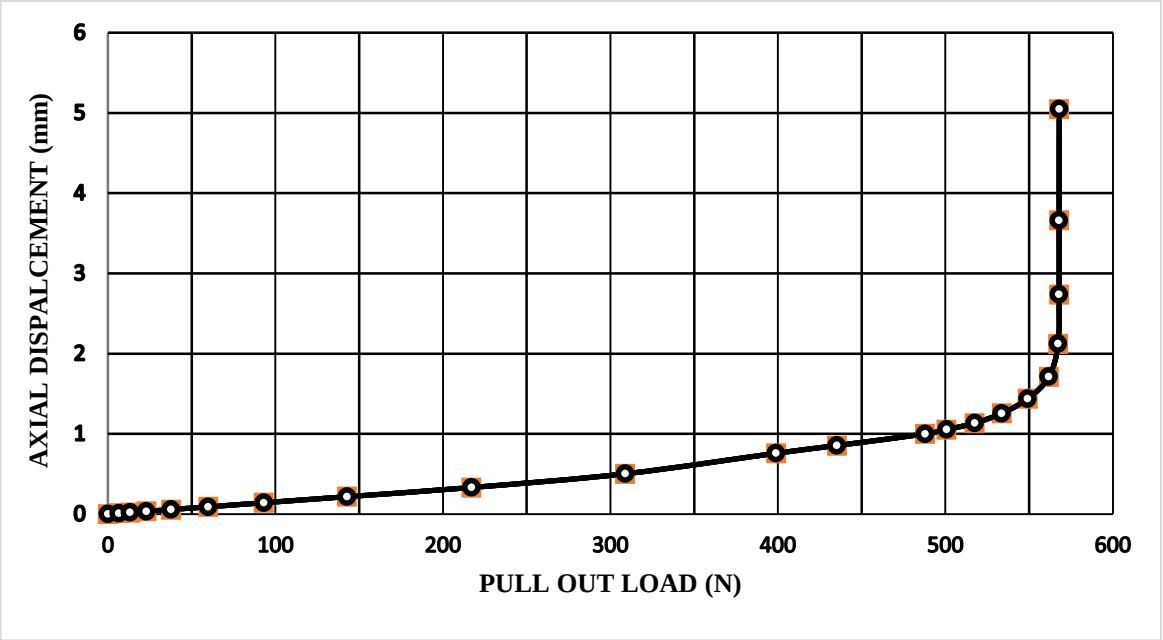

Fig. 6.1 Pull out Load vs. Axial displacement curve for
50 mm strip plate and embedment ratio 1

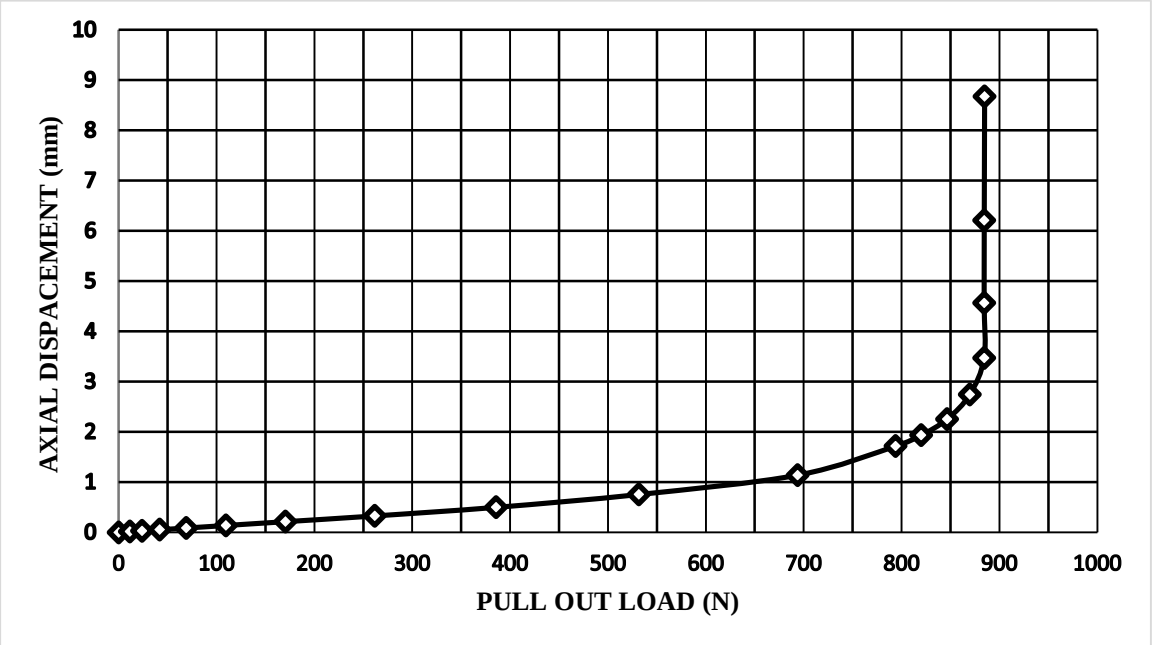

Fig. 6.3 Pull out Load vs. Axial displacement curve for
50 mm strip plate and embedment ratio 2

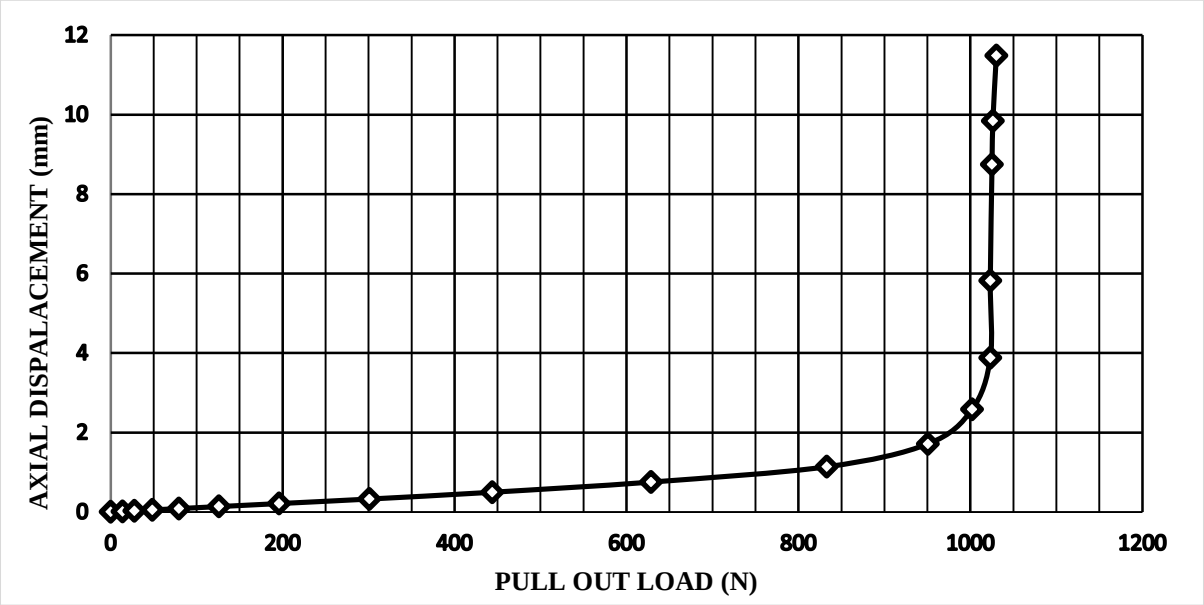

Fig. 6.3 Pull out Load vs. Axial displacement curve for
50 mm strip plate and embedment ratio 3

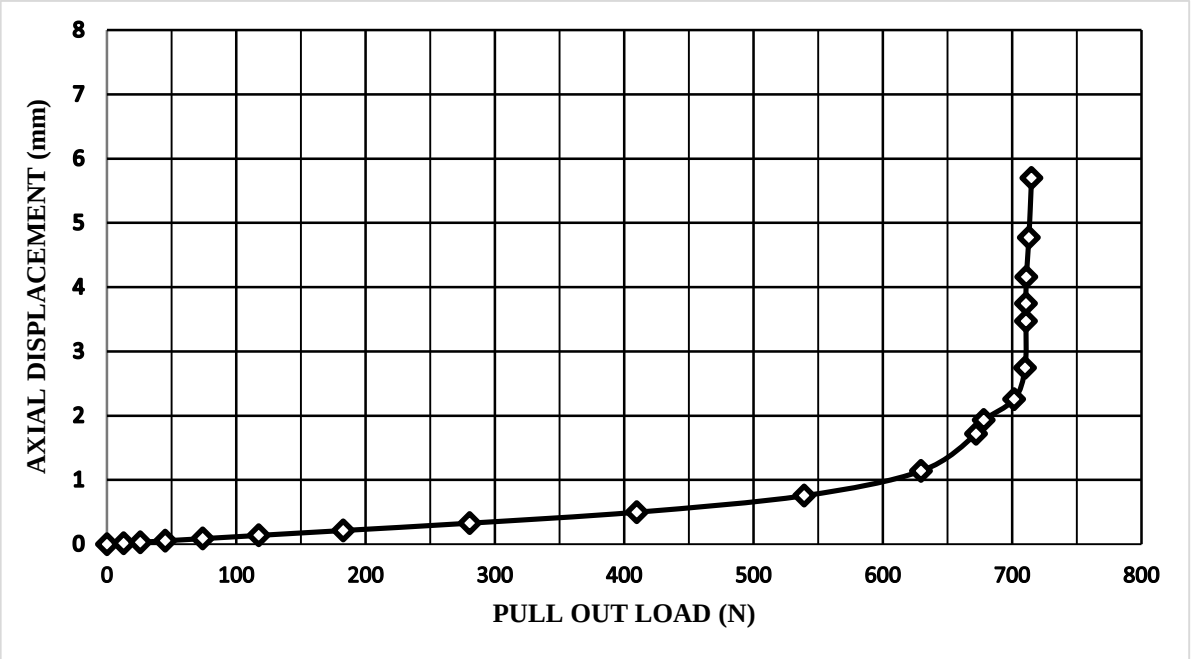

Fig. 6.4 Pull out Load vs. Axial displacement curve for
75 mm strip plate and embedment ratio 1

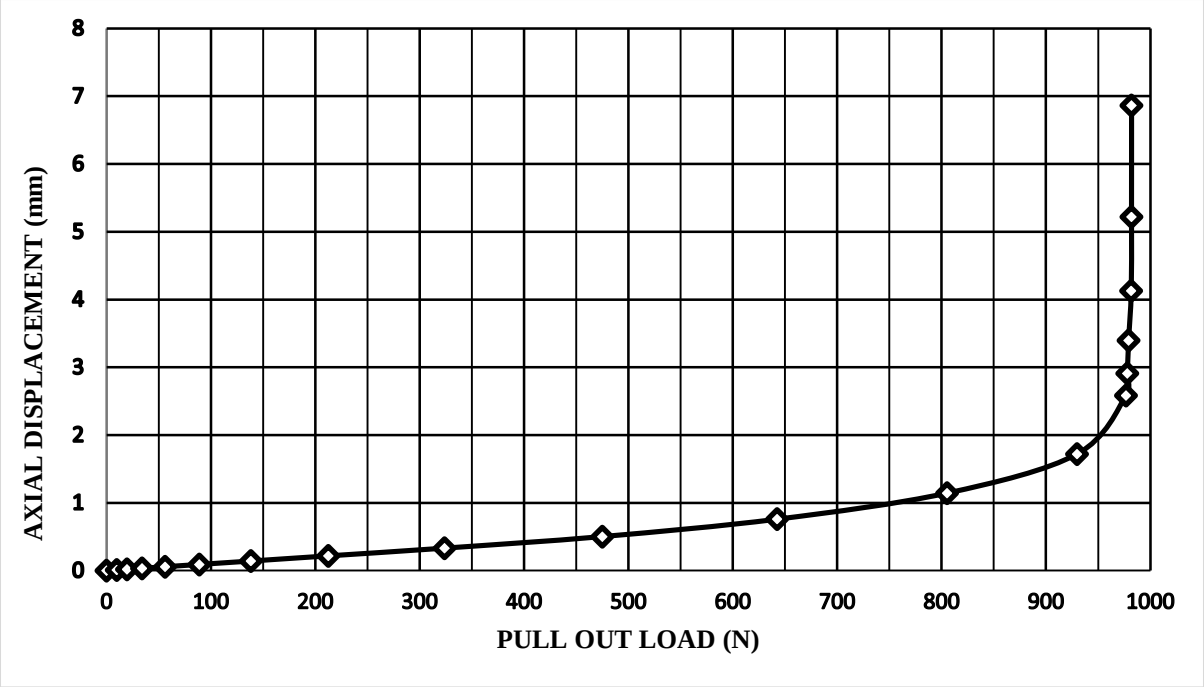

Fig. 6.4 Pull out Load vs. Axial displacement curve for
75 mm strip plate and embedment ratio 2

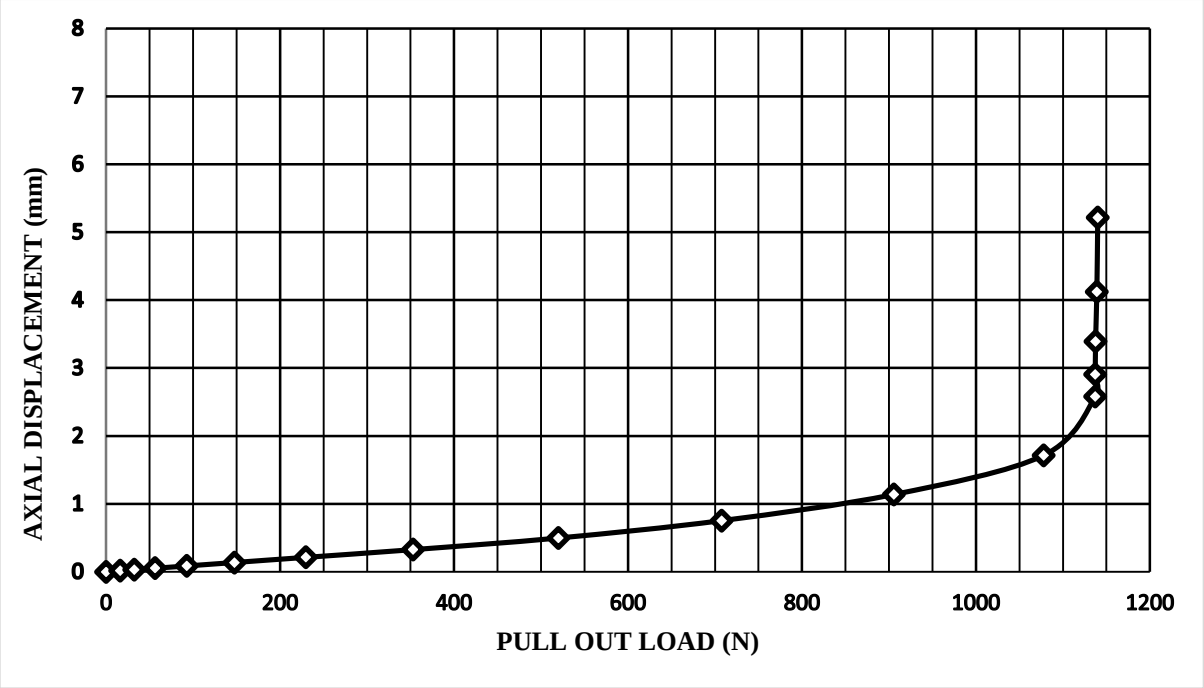

Fig. 6.4 Pull out Load vs. Axial displacement curve for
75 mm strip plate and embedment ratio 3

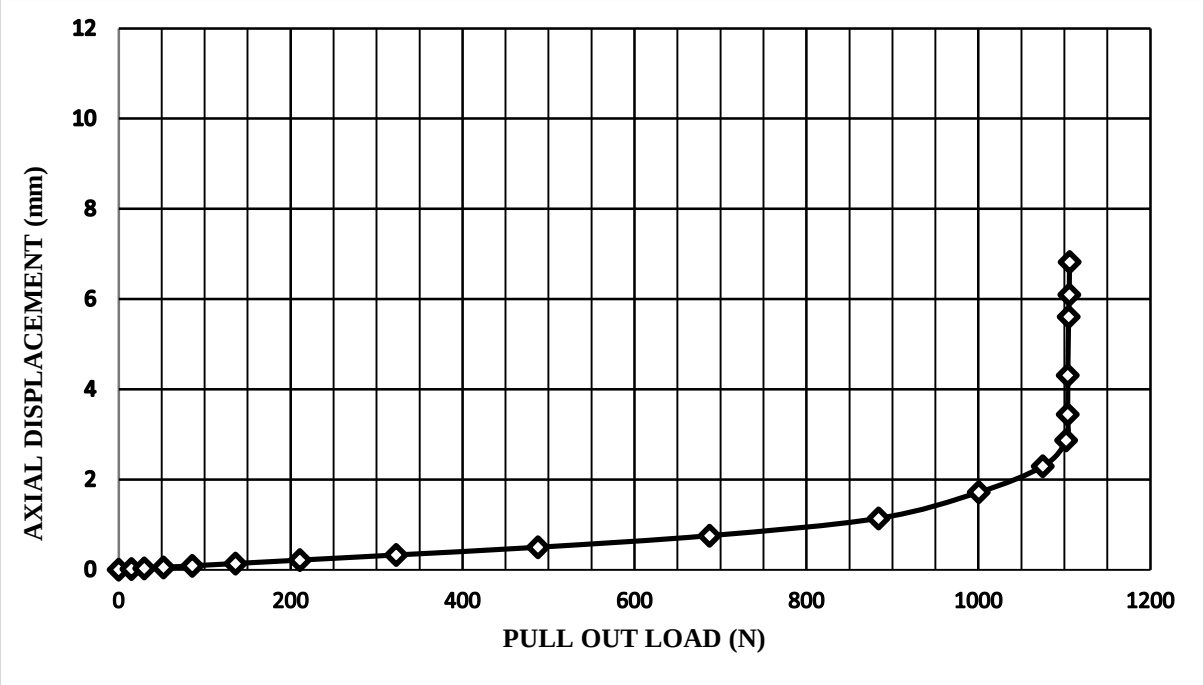

Fig. 6.7 Pull out Load vs. Axial displacement curve for
100 mm strip plate and embedment ratio 1

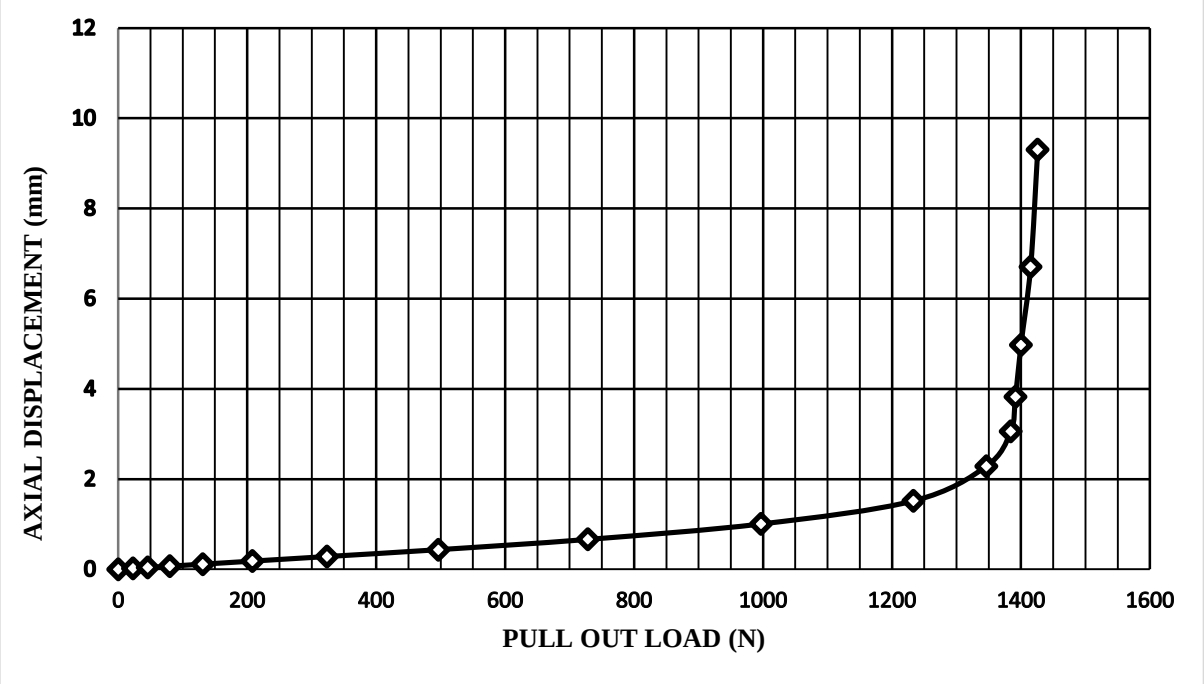

Fig. 6.8 Pull out Load vs. Axial displacement curve for
100 mm strip plate and embedment ratio 2

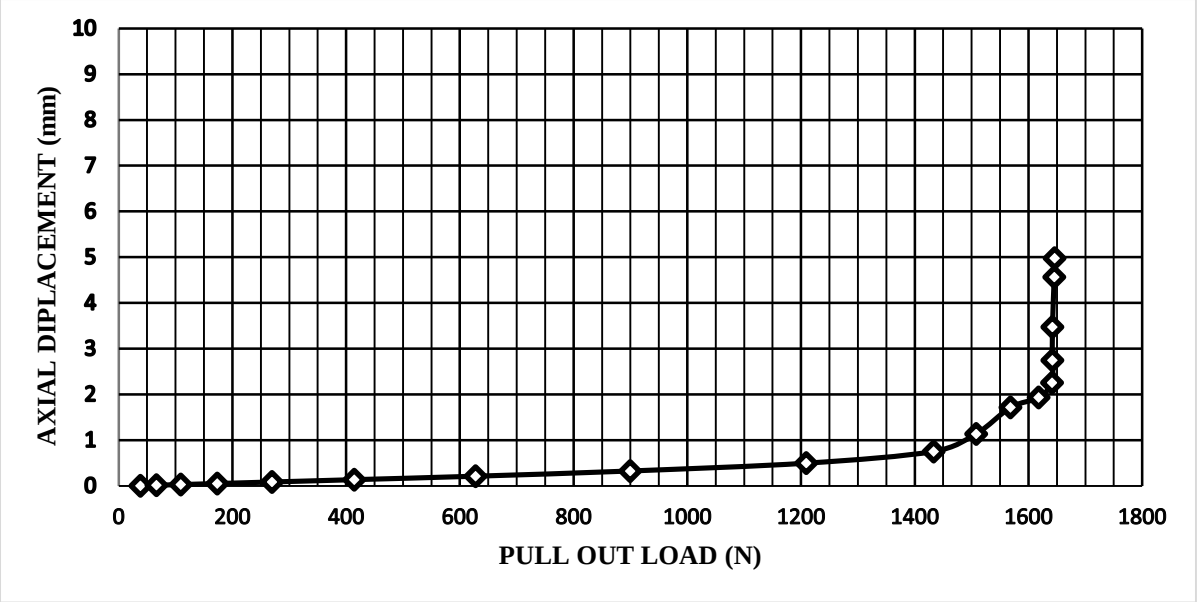

Fig. 6.9 Pull out Load vs. Axial displacement curve for
100 mm strip plate and embedment ratio 3

Table. 6.2 Ultimate Pull out loads and corresponding displacement

Sl. No.	Plate Anchor Size (B) mm	Embedment ratio (H/B)	Ultimate pullout capacity (Q_u) N	Corresponding Axial displacement (Δ) mm
1	50	1	567	2.12
2		2	884	3.47
3		3	978	3.88
4	75	1	710	2.74
5		2	978	2.90
6		3	1137	2.90
7	100	1	1104	3.44
8		2	1392	3.82
9		3	1641	3.47

6.4.2 Ultimate Pull Out capacity Vs. Plate Size

The values of ultimate pull out capacities have been plotted against plate width (B) values have been for a particular value of embedment ratio as shown in fig. 6.10.

It is observed from the figure that for a given embedment ratio, the ultimate pull out capacity increases with the plate size. This is due to involvement of more soil mass acting against pull out.

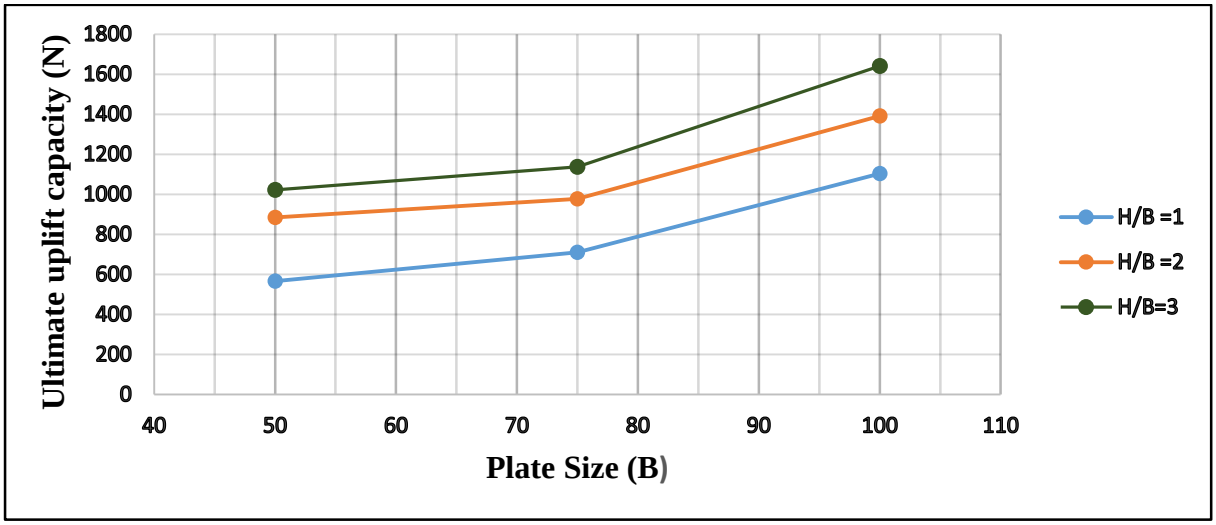

Fig. 6.10 Ultimate Pull out Capacity Vs. Plate Size for various embedment ratio

6.4.3 Ultimate Pull Out capacity Vs. Embedment ratio

The ultimate pull out capacities have been plotted with embedment ratio (H/B) for all cases, in fig. 6.11.

It is observed from the figure that ultimate pull out capacity increases with embedment ratio (H/B) for particular plate sizes. With higher plate size the value is more for a particular embedment ratio (H/B). The increase is prominent for increase of plate size for 75mm to 100 mm. This is probably due to the fact that considerable soil mass is getting involved in resisting uplift in case of 100mm wide plate.

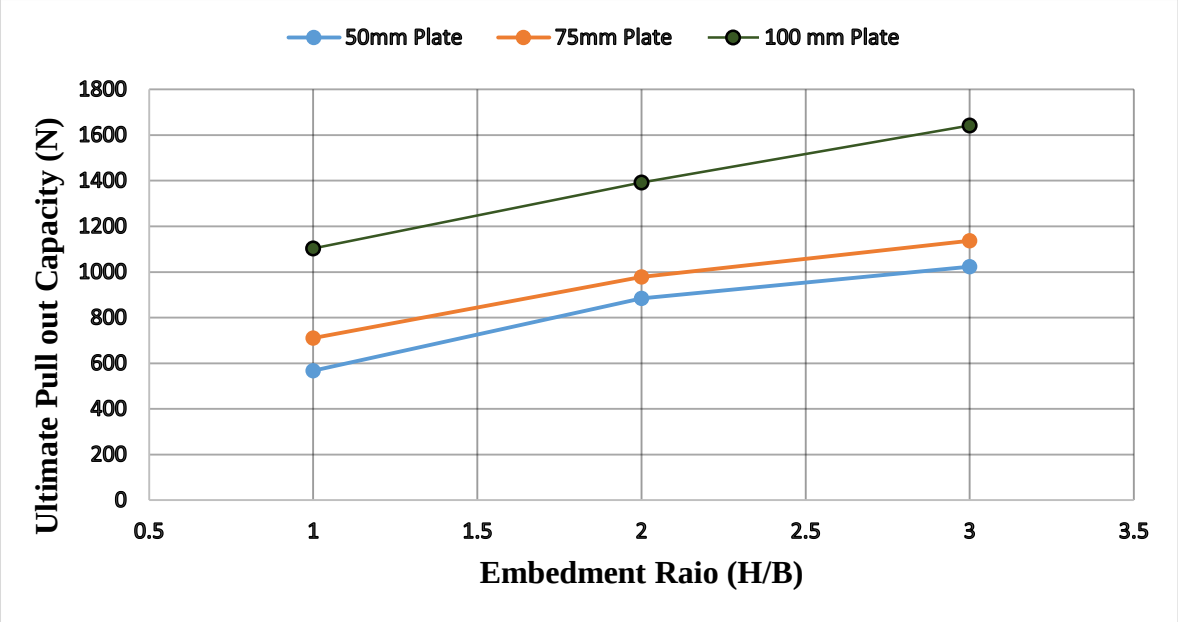

Fig. 6.11 Ultimate Pull out Capacity Vs. Embedment ratio for various Plate Sizes

6.4.4 Stress Contours

Stress contours for different plate sizes and different embedment ratios have been presented in fig. 6.12 to fig. 6.20.

Values of maximum stress developed in soil for each cases have been presented in table 6.3. It appears from table that, for each plate size, the value of maximum stress increases with increase of embedment ratio from 1 to 3. This is due to the fact that with increase of embedment ratio, more soil mass is getting affected in the vertical direction from the level of plate. It appears from the stress contours that the stress is reducing towards the top vertically as well as away from the plate horizontally in both directions. However it appears from stress contours that more soil mass is getting stressed with increase of embedment ratio as well as with increase of plate size. This phenomenon corroborates with the corresponding increase of pull out capacity with embedment ratio for a particular plate size.

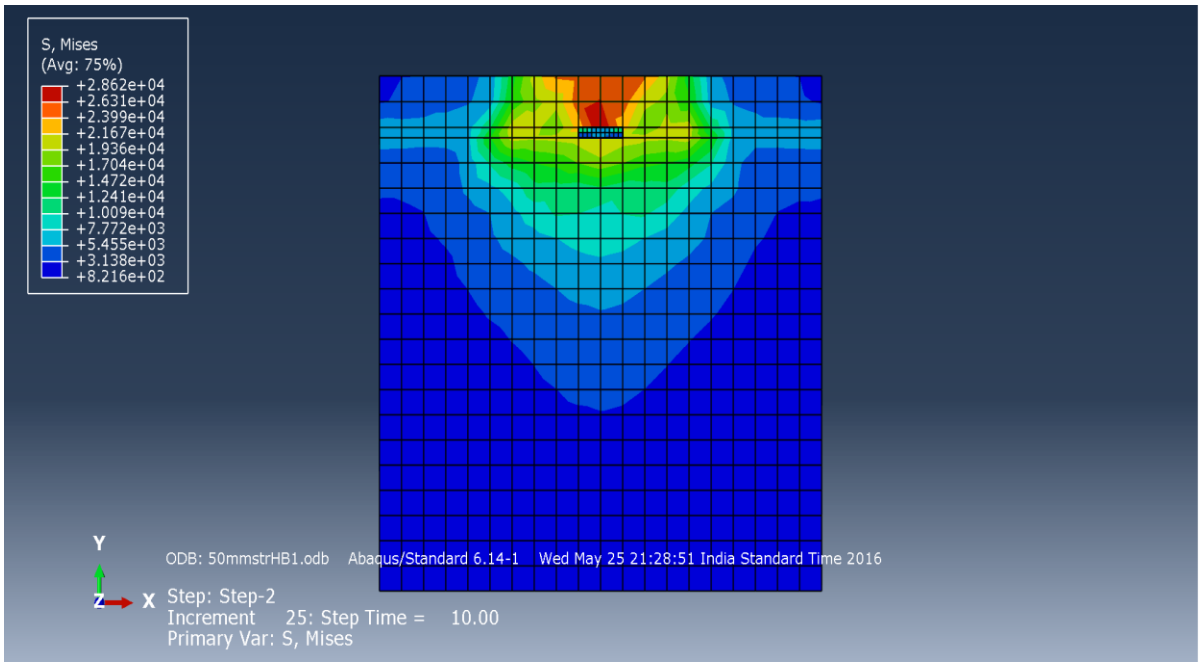

Fig. 6.12 Stress Contour of model for 50 mm strip plate and embedment ratio 1

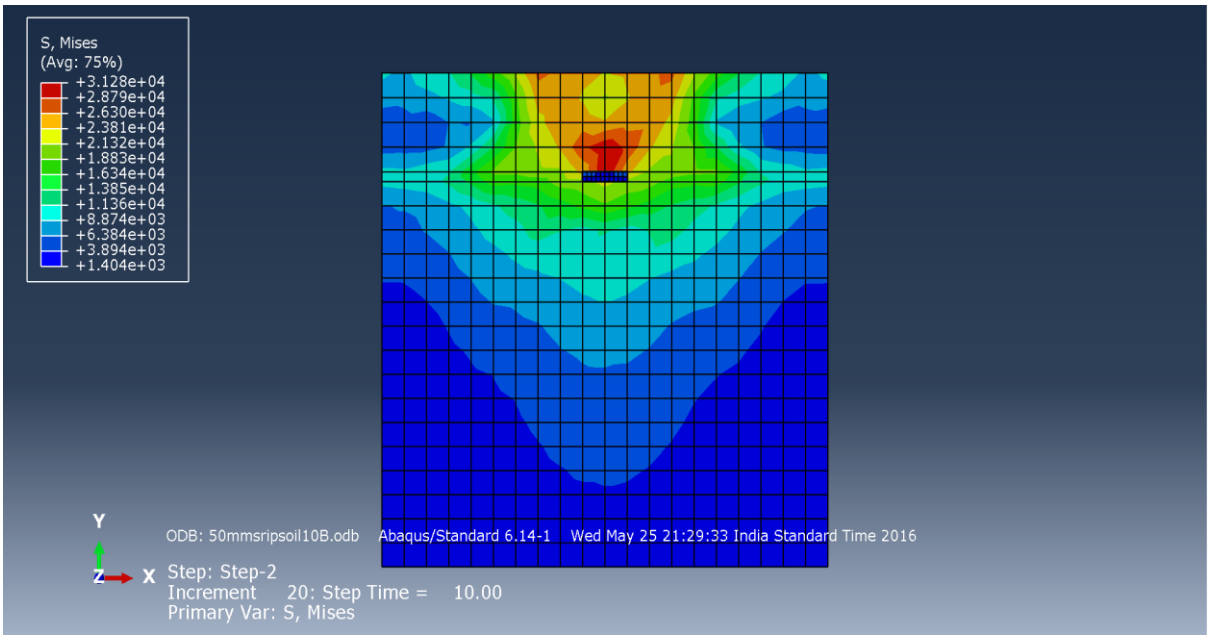

Fig. 6.13 Stress Contour of model for 50 mm strip plate and embedment ratio 2

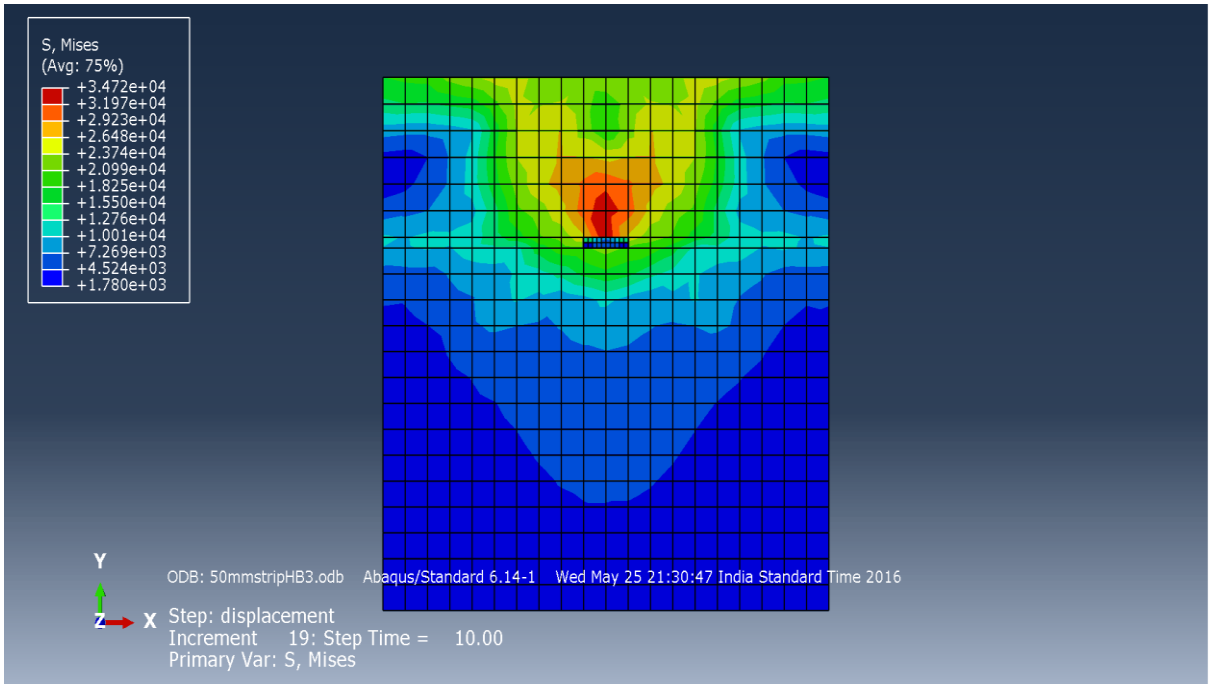

Fig. 6.14 Stress Contour of model for 50 mm strip plate and embedment ratio 3

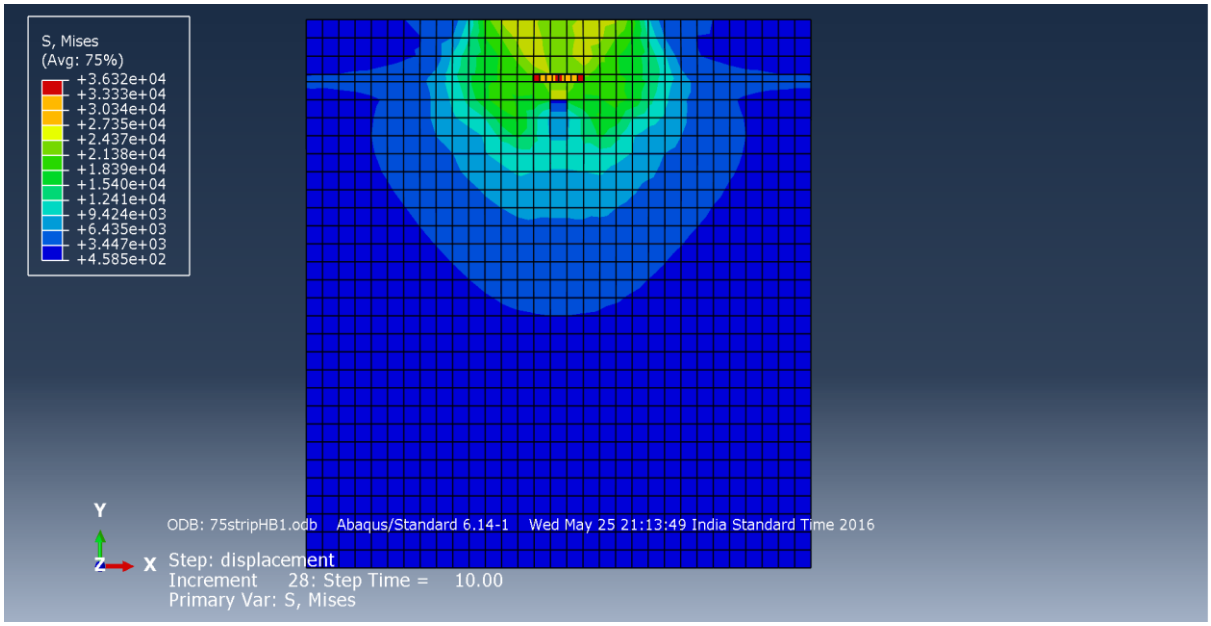

Fig. 6.15 Stress Contour of model for 75 mm strip plate and embedment ratio 1

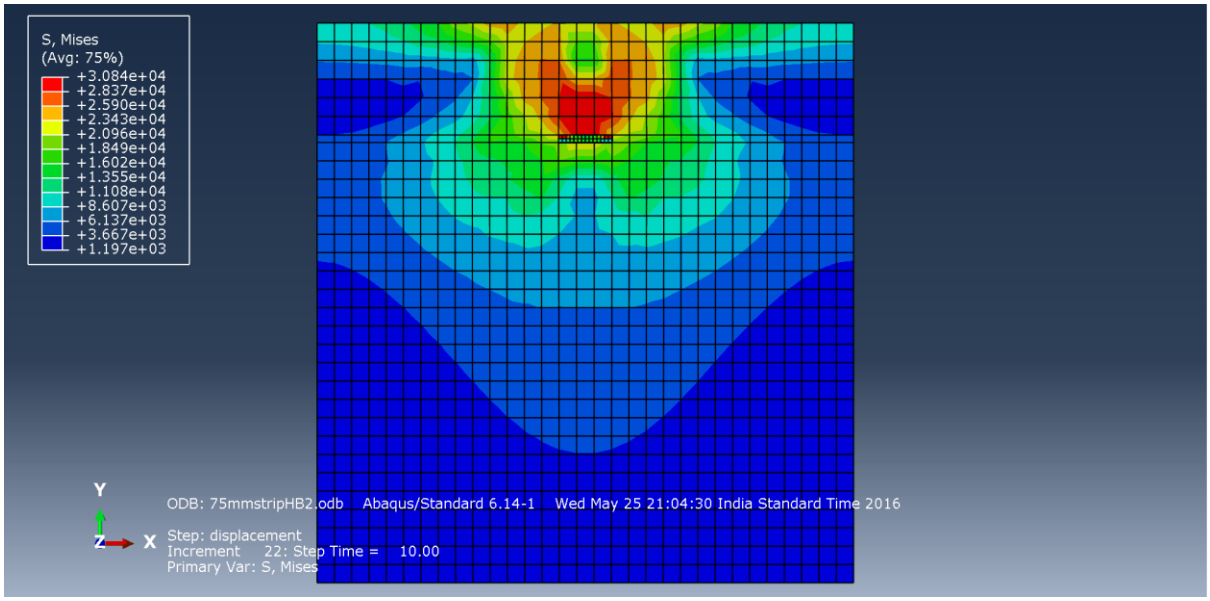

Fig. 6.16 Stress Contour of model for 75 mm strip plate and embedment ratio 2

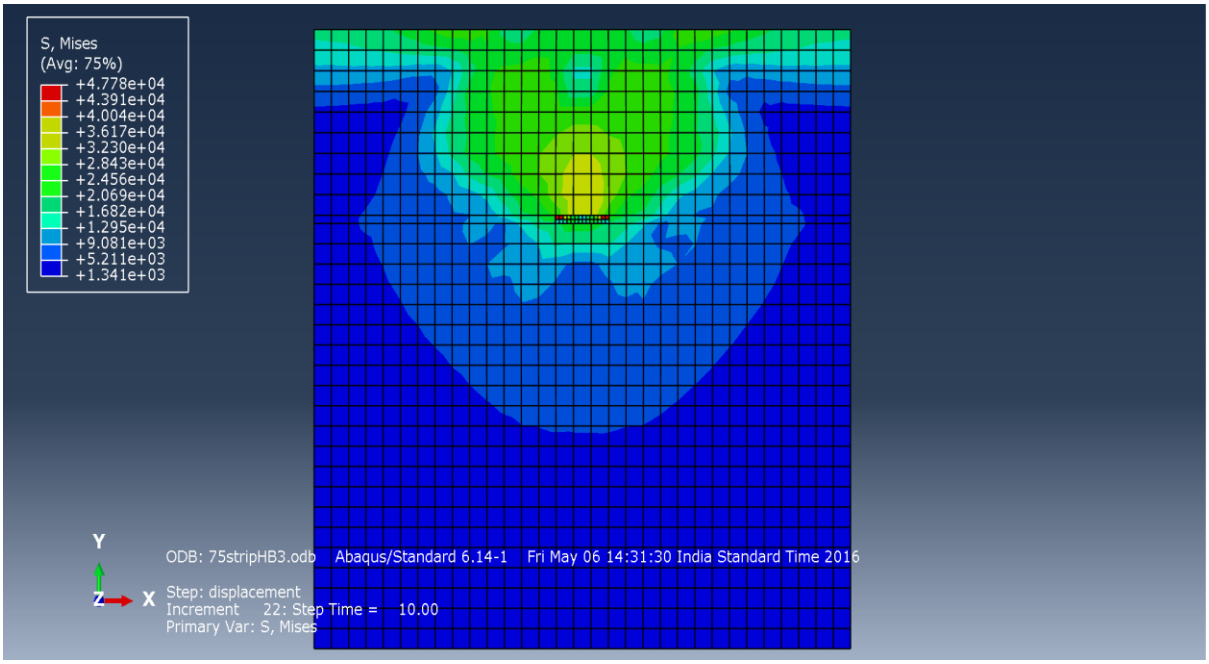

Fig. 6.17 Stress Contour of model for 75 mm strip plate and embedment ratio 3

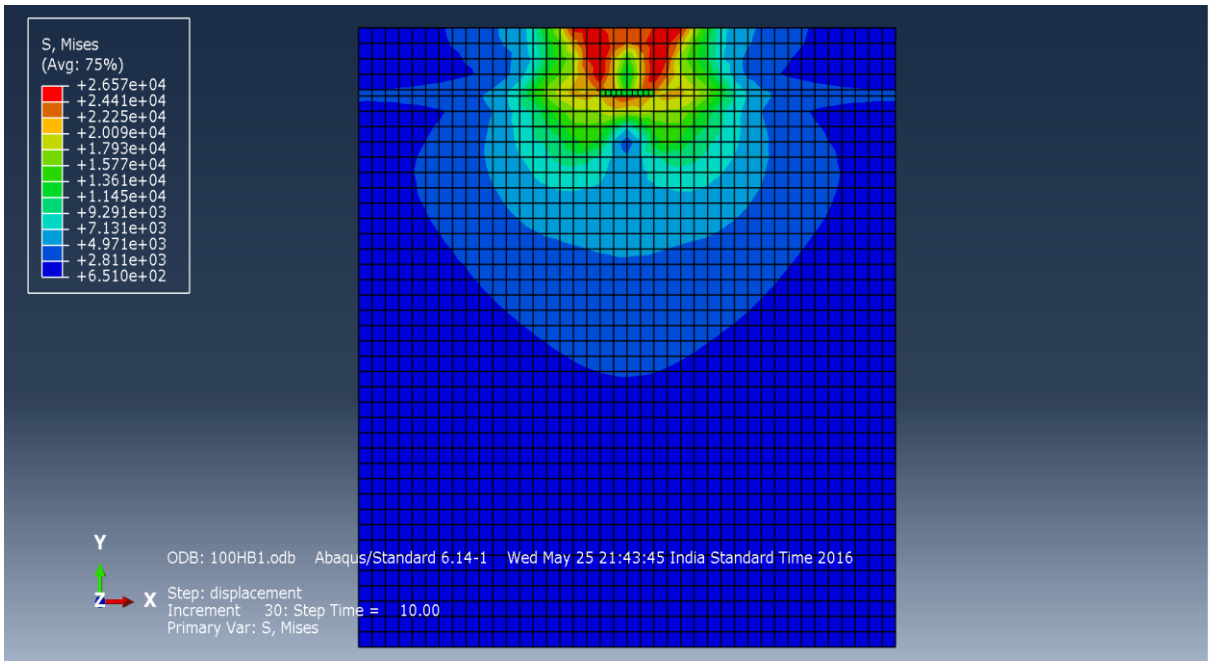

Fig. 6.18 Stress Contour of model for 100 mm strip plate and embedment ratio 1

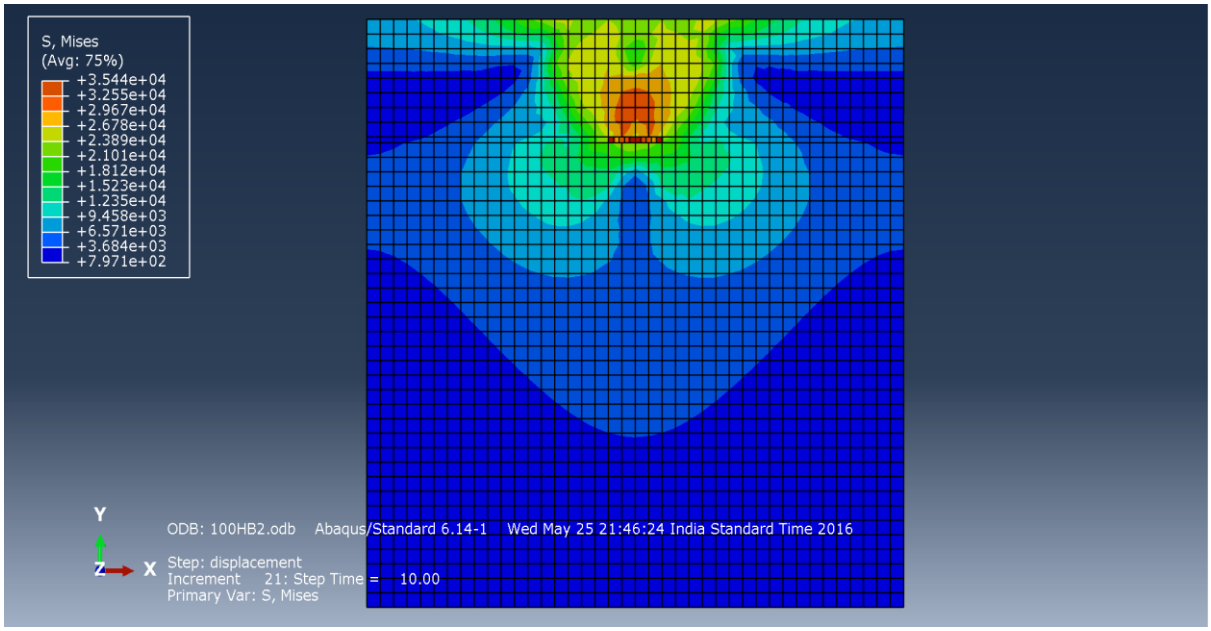

Fig. 6.19 Stress Contour of model for 100 mm strip plate and embedment ratio 2

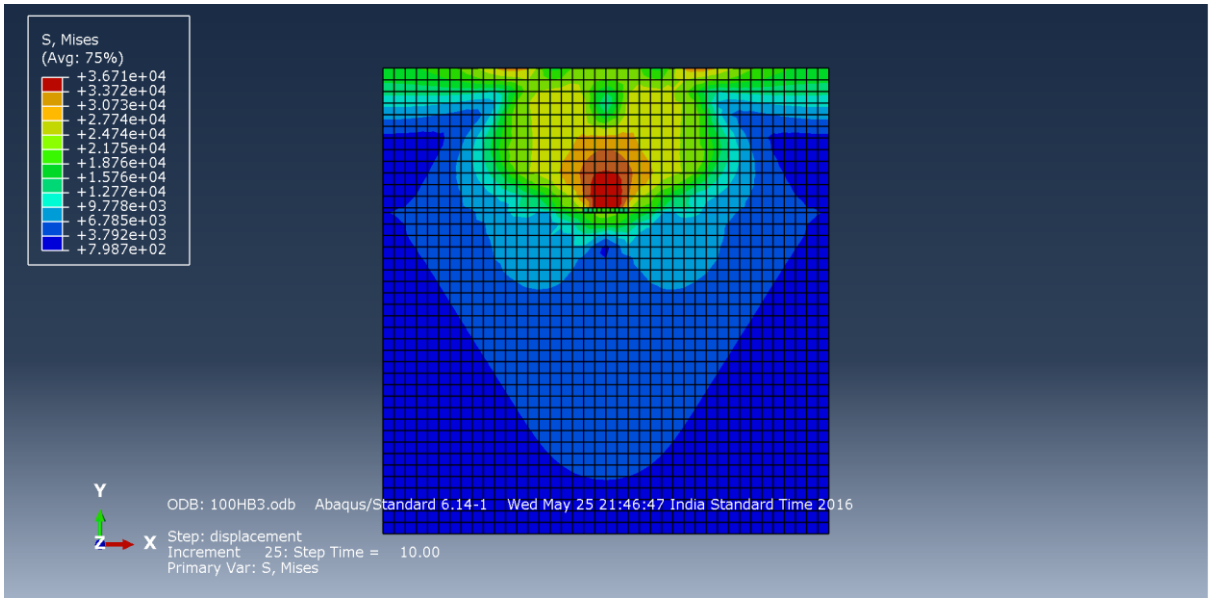

Fig. 6.20 Stress Contour of model for 100 mm strip plate and embedment ratio 3

Table. 6.3 Maximum Stress in soil

Sl. No.	Plate Size (B) in mm	Embedment Ratio (H/B)	Maximum Stress in soil (N/m^2)
1	50	1	2.862×10^4
2		2	3.128×10^4
3		3	3.472×10^4
4	75	1	3.034×10^4
5		2	3.084×10^4
6		3	3.617×10^4
7	100	1	2.657×10^4
8		2	3.255×10^4
9		3	3.671×10^4

Chapter – 7

SUMMARY, CONCLUSION & SCOPE OF FURTHER STUDY

7.1 SUMMARY

In order to study the behaviour of shallow strip anchors, embedded in clay a numerical study was carried out by finite element method using ABAQUS software. Numerical model of 50 mm, 75 mm and 100 mm wide plate anchors have been studied for embedment ratios of 1, 2 and 3. In this way a total number of nine cases have been studied. The load displacement curve and the stress contour for each case have been obtained from the output of the software. Both the load displacement curves and stress contours have been examined to study the behaviour of strip anchors.

7.2 CONCLUSIONS

The following conclusion may be drawn from present study

1. For a given embedment ratio, the ultimate pull out capacity increases with increase the plate size.
2. Ultimate pull out capacity increases with embedment ratio for a particular plate size. With higher plate size the value is more for a particular embedment ratio
3. For each plate size the value of maximum stress increases with increase of embedment ratio from 1 to 3.
4. the stress in soil reduces towards the top vertically and away from the plate horizontally in both direction

7.3 SCOPE OF FURTHER STUDY

From the study reported in this thesis, it appears that the research work may be carried out towards the following directions:

1. Numerical study of pull out behaviour of strip anchors in reinforced and unreinforced clayey soil.
2. The study may be extended for dynamic loading.
3. Similar laboratory studies may be carried out to supplement the numerical studies.

REFERENCES

Meyerhof .G.C and Adams (1968) "The Uplift Capacity of foundation" Canadian Geotechnical Journal Vol V No 4.

Das, B.M. (1978) Model tests for uplift capacity of foundation in clay, Soils and Foundation, Japan, 18(2) : 17-24.

Das, B.M. (1980) A procedure for estimation of ultimate capacity of foundation in clay, Soil and Foundation, Japan, 20(1): 77-82

Rowe. R. K and Davis. E. H (1982) "The behavior of anchor plates in sand" Geotech 32 NO. 1 , 25 – 41

Chattopadhyay B.C and Pise P.J (1986) "Uplift Capacity of pile in Sand", Journal of Geotechnical Engineering Division. ASCE, Vol. 112 No. 9

Saran, S., and Rao, P.P., (2002), 'Uplift behaviour of horizontal plate anchors with geosynthetics', Indian Geotechnical Journal, vol.32, No.2, pp.329-338.

Merifield, R.S. and Sloan, S.W. (2006), 'The ultimate pullout capacity of anchors in frictional soils', Canadian Geotechnical Journal, vol.43, pp.852-868.

Bhattacharya P., Bhowmik D, Mukherjee S. P., Chattopadhyay B. C. (2008), The 12th International Conference of International Association for Computer Methods and Advances in Geomechanics (IACMAG), 1-6 October, 2008, Goa, India :3441-3447

Merifield, R.S., Lyamin A.V., Sloan, S.W. and Yu, H.S. (2003), 'Three dimensional lower bound solutions for stability of plate anchors in clay', Journal of Geotechnical and Geo-environmental Engineering, ASCE, vol.129, No.3, pp.243-253

Niroumand, H. (2010) "Experimental Study of Horizontal Anchor Plates in Cohesive Soils", Electronic journal of geotechnical engineering (EJGE), Vol. 15, pp. 879 – 886

Bhattacharya P, Mukherjee S, Chattopadhyaya B. C (2010); PhD Thesis , Civil Engineering Department, Jadavpur University.

Mistri B and Singh B (2011) “Pullout behavior of plate anchors in cohesive soils”, Civil Engineering Department, IIT Guwahati, Guwahati Assam, India

SIMULIA ABAQUS 6.14 documentation

David M Potts Psktsa Nd Lidija Zdravkovic, Finite element analysis in geotechnical engineering, Imperial College of Science, Technology and Medicine

Hanna .A, Foriero. A and Ayadat. A (2014) Pullout Capacity of Inclined Shallow Single Anchor Plate in Sand , Indian Geotechnical Society

Suganya A and Arumairaj P.D. (2015) “Experimental study on behaviour of plate anchors in cohesionless soil” Govt.College of Technology, Coimbatore